

# A distant descendant of the six-vertex model

Vladimir V. Bazhanov<sup>1</sup> and Sergey M. Sergeev<sup>1,2</sup>

<sup>1</sup> Department of Fundamental and Theoretical Physics, Research School of Physics  
Australian National University, Canberra, ACT 2601, Australia

<sup>2</sup> Faculty of Science and Technology, University of Canberra, Bruce, ACT 2617,  
Australia

**Abstract.** In this paper we present a new solution of the star-triangle relation having positive Boltzmann weights. The solution defines an exactly solvable two-dimensional Ising-type (edge interaction) model of statistical mechanics where the local “spin variables” can take arbitrary integer values, i.e., the number of possible spin states at each site of the lattice is infinite. There is also an equivalent “dual” formulation of the model, where the spins take continuous real values on the circle. From algebraic point of view this model is closely related to the 6-vertex model. It is connected with the construction of an intertwiner for two infinite-dimensional representations of the quantum affine algebra  $U_q(\widehat{sl}(2))$  without the highest and lowest weights. The partition function of the model in the large lattice limit is calculated by the inversion relation method. Amazingly, it coincides with the partition function of the off-critical 8-vertex free-fermion model.

# 1 Introduction

There is an important class of integrable two-dimensional lattice models of statistical mechanics [1] with only a pair interaction between neighbouring spins, i.e., where two spins interact only if they are connected by an edge of the lattice. We will call them as “edge interaction” or “Ising-type” models. The commutativity of transfer matrices for these models can usually be derived from the star–triangle relation [2] which is a special form of the Yang-Baxter equation [3–5].

Over the past forty years a number of such models was discovered. The most notable discrete-spin models in this class include the Kashiwara-Miwa [6] and chiral Potts [7–9] models (both of them also contain the Ising model [2] and Fateev-Zamolodchikov  $Z_N$ -model [10] as particular cases) see [11] for a review. There are also important continuous spin models, including Zamolodchikov’s “fishing-net” model [12], which describes certain planar Feynman diagrams in quantum field theory, and the Faddeev-Volkov model [13], connected with quantization [14] of discrete conformal transformations [15, 16]. Quite interestingly, all solutions of the star-triangle relation associated with these models (both with discrete and continuous spin variables) can be obtained as special cases of a rather general “master solution” of this relation, which was found in [18].<sup>1</sup> Algebraically, the master solution is related to the modular double [19, 20] of the elliptic Sklyanin algebra [21] and Spiridonov’s elliptic beta integral [22].

In this paper we present yet another solution of the star-triangle relation, with positive Boltzmann weights, which, apparently, cannot be obtained from the master solution and its specializations (at least, to the authors’ knowledge). Our new solution involves spin variables taking arbitrary integer values  $-\infty < a, b < +\infty$ , and reflection-symmetric Boltzmann weights, which are unchanged upon interchanging the edge spins  $a, b$ . The weights depend on the absolute value of the spin difference,

$$W_x(a - b) = W_x(b - a) = x^{a-b} \frac{(-\mathbf{q}^{a-b+1} x^2; \mathbf{q}^2)_\infty}{(-\mathbf{q}^{a-b+1}/x^2; \mathbf{q}^2)_\infty}. \quad (1.1)$$

and a multiplicative spectral variable  $x$  (see how it enters the star-triangle relation (1.4) below). Here  $(x; \mathbf{q}^2)_\infty$  denotes the  $\mathbf{q}$ -Pochhammer symbol

$$(x; \mathbf{q}^2)_\infty = \prod_{k=0}^{\infty} (1 - x \mathbf{q}^{2k}), \quad (1.2)$$

involving a fixed parameter  $\mathbf{q}$ , such that  $|\mathbf{q}| < 1$ . It is convenient to also define the “crossing parameter”,

$$\xi = i\sqrt{\mathbf{q}}, \quad \mathbf{q} = -\xi^2. \quad (1.3)$$

We state that the above weights satisfy the star-triangle relation of the form,

$$\begin{aligned} \sum_{d \in \mathbb{Z}} W_{\xi/x}(a - d) W_{xy}(c - d) W_{\xi/y}(b - d) \\ = \mathcal{R} W_x(b - c) W_{\xi/(xy)}(a - b) W_y(a - c), \end{aligned} \quad (1.4)$$

where  $\mathcal{R}$  is an explicitly known scalar factor

$$\mathcal{R} = \kappa_s \frac{\sigma(x^2) \sigma(y^2)}{\sigma(x^2 y^2)}, \quad \sigma(x) = \frac{(-\mathbf{q}/x; \mathbf{q})_\infty}{(x; \mathbf{q})_\infty}, \quad \kappa_s = \frac{(\mathbf{q}; \mathbf{q})_\infty}{(-\mathbf{q}; \mathbf{q})_\infty}, \quad (1.5)$$

which depends on the spectral variables  $x$  and  $y$ , but is independent of the spins  $a, b, c \in \mathbb{Z}$ . It is important to note that if the parameter  $\xi$  in (1.3) and the spectral variables  $x$  and  $y$  are real and belong to the domain

$$0 < \xi < 1, \quad \xi < x, y, xy < 1, \quad (1.6)$$

---

<sup>1</sup>To be more precise, the “master solution” only contains the solutions, which have a single one-dimensional spin at each lattice site. For this reason, it cannot contain the  $D \geq 2$  fishing-net model which has multi-dimensional spins.

then all weights entering (1.4) are *real and positive*. Note also, that for large  $n$  the expression inside the sum in (1.4) behaves as  $O(q^{|n|})$ , so for  $|q| < 1$  the sum always converges as a geometric series.

Let us briefly explain how the above results were obtained. The Boltzmann weights (1.1) originate from the calculation of the  $R$ -matrix intertwining two particular infinite-dimensional representations of the quantum affine algebra  $U_q(\widehat{sl}(2))$ . These representations do not have the highest and lowest weights and their Cartan elements are realized as shift operators. A similar problem, but for the case of cyclic representations of  $U_q(\widehat{sl}(2))$ , with  $q$  being a root of unity, has been previously considered in [23]. Following the results of that work one would expect that the matrix elements of the intertwining  $R$ -matrix in our case factorize into a product of four factors depending on two spins only. Indeed, our analysis exactly confirms such factorization. In particular, the associated two-spin weights  $W_x(a-b)$  are determined by the following recurrence

$$\frac{W_x(n)}{W_x(n-2)} = \frac{x^2 + q^{n-1}}{1 + q^{n-1}x^2}, \quad n \in \mathbb{Z}, \quad (1.7)$$

and inversion relations,

$$\sum_{n \in \mathbb{Z}} W_{\xi x}(a-n) W_{\xi/x}(n-b) \simeq \delta_{a,b}, \quad a, b, n \in \mathbb{Z}, \quad (1.8)$$

where  $\xi$  is defined in (1.3) and the symbol  $\simeq$  means the proportionality up to a scalar factor independent of spins. Notice, that the relation (1.7) is a *second order* recurrence relation, which do not allow to determine  $W_x(n)$  without additional information. For instance, starting from the value of  $W_x(0)$  one can only calculate the values of  $W_x(n)$  for even  $n = \pm 2, \pm 4, \dots$ , however, in order to calculate them for odd  $n = \pm 1, \pm 3, \dots$ , one needs to specify another initial value, say  $W_x(1)$ . Both  $W_x(0)$  and  $W_x(1)$  are not just constants, but functions of the spectral variable  $x$ , and only one of them could be absorbed into the overall normalization of  $W_x(n)$ .

The above ‘‘odd-even’’ problem is, in fact, well known [24] in connection with the chiral Potts model (though in that case it is slightly simpler, because, when  $q$  is a root of unity, the values of spins are identified *modulo* some integer  $N$ ,  $N \geq 2$ , and, therefore, can only take a finite number of values  $n \in \mathbb{Z}_N$ ).<sup>2</sup> The resolution of this problem, suggested in [25], essentially reduces to an exclusion of odd numbers from all consideration. Technically this is achieved by the replacement  $n \rightarrow 2n$  which transforms (1.7) into a first order recurrence for  $W$ . Unfortunately, the above recipe does not work in our  $|q| < 1$  case, since the weights  $W_x(n)$ , obtained in this way, do not satisfy the inversion relation (1.8) (despite satisfying it in the root of unity case).

In our approach we retain the second order recurrence relation in the original form (1.7) and substitute its most general solution, including two unknown functions  $W_x(0)$  and  $W_x(1)$ , into the inversion relation (1.8). Remarkably, this relation allows one to uniquely fix the weights  $W_x(n)$  (to within an overall normalization and some trivial equivalence transformation factors). The result is given in (1.1). The handling of the inversion relation (1.8) is based on some important extensions of the Ramanujan  ${}_1\psi_1$  bilateral summation formula [26].

Initially, we have obtained the star-triangle relation (1.4) by the perturbation theory around the point  $xy = 1$  (where (1.4) reduces to the inversion relation (1.8)) and then thoroughly verified it by numerical calculations. Subsequently, but rather accidentally, we have realized that the star-triangle relation (1.4) could be deduced from the ‘‘*constant beta pentagon equation for the circle locally compact Abelian group  $\mathbb{T}$* ’’, by Garoufalidis and Kashaev [27]. Evidently, the connection is far from being obvious but, certainly, worth to be explored further.

As is well known [1] every solution of the star-triangle relation can be used to define exactly solvable edge interaction models on various two-dimensional lattices. For purposes of this introduction it is enough to consider an homogeneous square lattice. In this case the partition function reads

$$Z = \sum_{a_m \in \mathbb{Z}} \prod_{(ij)} (\rho(x) W_x(a_i - a_j)) \prod_{(kl)} (\rho(\xi/x) W_{\xi/x}(a_k - a_l)) \quad (1.9)$$

---

<sup>2</sup>Actually, the problem only arises for even values of  $N$ , since for odd  $N$  the second order recurrence (1.7) covers all elements of the set  $\mathbb{Z}_N$  due to the cyclic symmetry.

where the first product is taken over all horizontal edges ( $ij$ ), the second over all vertical edges ( $kl$ ) and the sum is taken over the spins  $\{a_m\}$  on interior sites of the lattice. The boundary spins are assumed to be fixed. In writing (1.9) we have included arbitrary normalization factors  $\rho(x)$  and  $\rho(\xi/x)$ , which might be imposed by the physical interpretation of the model. However, to keep the formulae more readable we prefer to drop these factors for the most of our considerations, only restoring them when necessary.

Note that, since the edge weights in (1.9) depend on spin differences, there exist an equivalent “dual” formulation of the model. It is also a square lattice edge-interaction model, where the spins take continuous real values on the circle  $0 \leq \phi_i, \phi_j < 2\pi$ . The corresponding weights  $\overline{W}_{\xi/x}(\phi_i - \phi_j)$ ,  $\overline{W}_x(\phi_k - \phi_l)$  for the horizontal and vertical edges are real and positive for  $0 < \xi < x < 1$ . They are defined by the Fourier transform,

$$\overline{W}_x(\varphi) = \kappa_s^{-1} \sigma(x^2) \sum_{n \in \mathbb{Z}} W_x(n) e^{i\varphi n} = \sigma(xe^{i\phi}) \sigma(xe^{-i\phi}), \quad (1.10)$$

where  $\kappa_s$  and  $\sigma(x)$  are given in (1.5). In the dual formulation the star-triangle relation (1.4) becomes a concise integral identity

$$\frac{1}{2\pi i} \oint \frac{dw}{w} \prod_{j=1}^3 \frac{\sigma(u_j w)}{\sigma(v_j w)} = \kappa_s \prod_{j=1}^3 \prod_{k=1}^3 \sigma(v_j/u_k)^{-1}, \quad \frac{v_1 v_2 v_3}{u_1 u_2 u_3} = \mathbf{q}^2, \quad (1.11)$$

where the integration contour is such that

$$\max(|\mathbf{q}/v_j|) < |w| < \min(|1/u_j|). \quad (1.12)$$

Here  $\{u_j\}$  and  $\{v_j\}$  are complex numbers, satisfying the constraints shown above, but otherwise arbitrary. Recalling that each function  $\sigma(x)$  is a ratio of two  $\mathbf{q}$ -Pochhammer symbols, the numerator and denominator of the integrand in (1.11) each contains products of six  $\mathbf{q}$ -Pochhammer symbols.

Using the inversion relation method [34–36] we calculate the partition function (1.9) of the model for the main physical regime  $0 < \xi < x < 1$  in a large lattice limit. Surprisingly, it coincides with the partition function of the off-critical 8-vertex model [5] at the free-fermion point.

The organization of the paper is as follows. In Sect.2 we consider the problem of constructing of  $R$ -matrices, intertwining some particular infinite-dimensional representations of the quantum affine algebra  $U_{\mathbf{q}}(\widehat{sl}(2))$  and derive a set of equation defining such  $R$ -matrices. In Sect.3 we solve these equations using the ideas of factorized  $R$ -matrices and the “face-vertex” correspondence. In Sect.4 we review the theory of solvable lattice models on arbitrary planar graphs. In Sect.5 we calculate the partition function of the model in the thermodynamic limit. In Conclusion we discuss the main results and indicate some directions for a future research.

## 2 Yang-Baxter equations

We start with the standard  $R$ -matrix of the 6-vertex model,

$$\begin{aligned} \mathcal{R}^{(6v)}(\mu)_{++}^{++} &= \mathcal{R}^{(6v)}(\mu)_{--}^{--} = \mu \mathbf{q} - \mu^{-1} \mathbf{q}^{-1}, \\ \mathcal{R}^{(6v)}(\mu)_{+-}^{+-} &= \mathcal{R}^{(6v)}(\mu)_{-+}^{-+} = \mathbf{q} - \mathbf{q}^{-1}, \\ \mathcal{R}^{(6v)}(\mu)_{+-}^{+ -} &= \mathcal{R}^{(6v)}(\mu)_{-+}^{- +} = \mu - \mu^{-1}, \end{aligned} \quad (2.1)$$

and the Yang-Baxter equation (YBE) defining the  $\mathbf{L}$ -operator

$$\sum_{j_1, j_2 = \pm 1} \mathbf{L}(\mu_1)_{i_1}^{j_1} \mathbf{L}(\mu_2)_{i_2}^{j_2} \mathcal{R}^{(6v)}(\mu_2/\mu_1)_{j_1, j_2}^{k_1, k_2} = \sum_{j_1, j_2 = \pm 1} \mathcal{R}^{(6v)}(\mu_2/\mu_1)_{i_1, i_2}^{j_1, j_2} \mathbf{L}(\mu_2)_{j_2}^{k_2} \mathbf{L}(\mu_1)_{j_1}^{k_1}, \quad (2.2)$$

where the matrix indices  $i_1, i_2, k_1, k_2$ , take two values  $\pm 1$  and  $q$  is a fixed parameter, such that  $|q| < 1$ . The operator  $\mathbf{L}(\mu)$  is a two-by-two matrix whose elements are operators acting in the “quantum space” and  $\mu$  is the “spectral variable”. Below we will often use the “crossing parameter”, defined as

$$\xi = i\sqrt{q}, \quad q = -\xi^2. \quad (2.3)$$

For the simplest  $\mathbf{L}$ -operator, which is a first order Laurent polynomial in the spectral variable  $\mu$ ,

$$\mathbf{L}(\mu) = \begin{pmatrix} \mu K - \mu^{-1} K^{-1} & F \\ E & \mu K^{-1} - \mu^{-1} K \end{pmatrix} \quad (2.4)$$

the YBE (2.2) just reduces to the defining relations of the quantum universal enveloping algebra  $U_q(sl(2))$ ,

$$K E = q E K, \quad K F = q^{-1} E K, \quad [E, F] = (q - q^{-1})(K^2 - K^{-2}). \quad (2.5)$$

Thus any of its representations leads to a solution of (2.2). Consider a particular infinite-dimensional representation  $\pi_s$  of this algebra, depending on the parameter  $s$ ,

$$\pi_s: \quad \pi_s[K] = \mathbf{V}, \quad \pi_s[E] = \mathbf{U}^{-1}(s \mathbf{V}^{-1} - s^{-1} \mathbf{V}), \quad \pi_s[F] = \mathbf{U}(s \mathbf{V} - s^{-1} \mathbf{V}^{-1}), \quad (2.6)$$

defined by the action of the operators  $\mathbf{U}$  and  $\mathbf{V}$  on the infinite set of basis vectors  $|a\rangle$ ,  $a \in \mathbb{Z}$ ,

$$\mathbf{U} \mathbf{V} = q \mathbf{V} \mathbf{U}, \quad (\mathbf{U})_{a,a'} = q^a \delta_{a,a'}, \quad (\mathbf{V})_{a,a'} = \delta_{a,a'+1}, \quad a, a' \in \mathbb{Z}. \quad (2.7)$$

Note, that the Cartan element  $\pi_s[K] = \mathbf{V}$  for this representation is realized as the shift operator. The  $\mathbf{L}$ -operator (2.4) then takes the form

$$\mathbf{L}(\mu | s) = \pi_s[\mathbf{L}(\mu)] = \begin{pmatrix} \mu \mathbf{V} - \mu^{-1} \mathbf{V}^{-1} & \mathbf{U}(s \mathbf{V} - s^{-1} \mathbf{V}^{-1}) \\ \mathbf{U}^{-1}(s \mathbf{V}^{-1} - s^{-1} \mathbf{V}) & \mu \mathbf{V}^{-1} - \mu^{-1} \mathbf{V} \end{pmatrix} \quad (2.8)$$

Now take two such  $\mathbf{L}$ -operators

$$\mathbf{L}_1 = \mathbf{L}_1(\mu_1 | s_1) = \pi_{s_1}[\mathbf{L}(\mu_1)], \quad \mathbf{L}_2 = \mathbf{L}_2(\mu_2 | s_2) = \pi_{s_2}[\mathbf{L}(\mu_2)]. \quad (2.9)$$

associated with two different representations  $\pi_{s_1}$  and  $\pi_{s_2}$ , labelled by the subscripts 1 and 2. Consider the problem of construction of an intertwining operator

$$\mathbf{S}_{12} = \mathbf{S}_{12}(\mu_1/\mu_2 | s_1, s_2), \quad (2.10)$$

which acts in the tensor product  $\pi_{s_1} \otimes \pi_{s_2}$  and satisfies the YBE

$$\begin{aligned} & \left( \mathbf{L}_1(\mu_1 | s_1) \circ \mathbf{L}_2(\mu_2 | s_2) \right) \mathbf{S}_{12}(\mu_1/\mu_2 | s_1, s_2) = \\ & = \mathbf{S}_{12}(\mu_1/\mu_2 | s_1, s_2) \left( \mathbf{L}_2(\mu_2 | s_2) \circ \mathbf{L}_1(\mu_1 | s_1) \right). \end{aligned} \quad (2.11)$$

Here the “circle-product” notation  $(\mathbf{L}_1 \circ \mathbf{L}_2)$  denotes the matrix product in the two-dimensional space and the tensor product in the infinite-dimensional quantum space  $\pi_{s_1} \otimes \pi_{s_2}$ . It is useful to view (2.11) as defining relations of the Yang-Baxter algebra realizing permutations of factors in the circle-products of  $\mathbf{L}$ -operators, by similarity transformations in the quantum space. Then, as is well known, the associativity condition for this algebra reduces to the YBE for intertwining operator  $\mathbf{S}$ ,

$$\mathbf{S}_{12} \mathbf{S}_{13} \mathbf{S}_{23} = \mathbf{S}_{23} \mathbf{S}_{13} \mathbf{S}_{12}, \quad (2.12)$$

where for brevity we have omitted (rather obvious) arguments of  $\mathbf{S}_{ij}$ .

Clearly, the above ‘‘permutation theory’’ interpretation of (2.11) requires some additional consistency relations, which we call the inversion relations. The first of them reads

$$\mathbf{S}_{12}(\mu_1/\mu_2 | s_1, s_2) \mathbf{S}_{21}(\mu_2/\mu_1 | s_2, s_1) \simeq \mathbf{I} \quad (2.13)$$

where the RHS is proportional to the unit operator in  $\pi_{s_1} \otimes \pi_{s_2}$  to within a scalar factor. The above relation is a simple corollary of fact that a permutation followed by the inverse permutation

$$(\mathbf{L}_1 \circ \mathbf{L}_2) \rightarrow (\mathbf{L}_2 \circ \mathbf{L}_1) \rightarrow (\mathbf{L}_1 \circ \mathbf{L}_2), \quad (2.14)$$

should reduce to the identity transformation. Indeed, using (2.11) twice, it is easy to see that the products  $(\mathbf{L}_1 \circ \mathbf{L}_2)$  and  $(\mathbf{L}_2 \circ \mathbf{L}_1)$  commute with the LHS of (2.13). Therefore, the latter must be proportional to the unit operator, otherwise the whole scheme becomes inconsistent. To obtain the second relation, define the inverse  $\mathbf{L}$ -operator

$$\mathbf{L}_1(\mu_1 | s_1) \mathbf{L}_1(\mu_1 | s_1)^{-1} = \mathbf{I} \quad (2.15)$$

where the product in the LHS implies both the matrix product in the two-dimensional space and the operator product in the quantum space  $\pi_{s_1}$ . The symbol  $\mathbf{I}$  here denotes the unit operator in both spaces. Now, let us multiply each side of (2.11) by  $\mathbf{L}_1(\mu_1 | s_1)^{-1}$  both from the left and from the right. Transposing the resulting equation in the space  $\pi_{s_1}$ , one obtains

$$\begin{aligned} \left( \mathbf{L}_2(\mu_2 | s_2) \circ \mathbf{L}_1(\tilde{\mu}_1 | \tilde{s}_1) \right) \mathbf{S}_{12}(\mu_1/\mu_2 | s_1, s_2)^{t_1} = \\ = \mathbf{S}_{12}(\mu_1/\mu_2 | s_1, s_2)^{t_1} \left( \mathbf{L}_1(\tilde{\mu}_1 | \tilde{s}_1) \circ \mathbf{L}_2(\mu_2 | s_2) \right) \end{aligned} \quad (2.16)$$

where

$$\tilde{\mu}_1 = \mu_1 \mathbf{q}^{-1}, \quad \tilde{s}_1 = s_1^{-1} \mathbf{q}^{-1}, \quad (2.17)$$

where the superscript  $t_1$  denotes the transposition in the space  $\pi_{s_1}$ . Here we have used the relation

$$\left( \mathbf{L}_1(\mu_1 | s_1)^{-1} \right)^{t_1} = \frac{1}{[\mu_1 s_1][\mu_1/(s_1 \mathbf{q})]} \mathbf{L}_1(\tilde{\mu}_1 | \tilde{s}_1), \quad [x] = x - x^{-1}, \quad (2.18)$$

which was obtained by a straitforward calculation from (2.4), (2.6) and (2.7). Now taking (2.16) and repeating the arguments that have led to (2.13) one obtains the second inversion relation

$$\mathbf{S}_{12}(\mu_1/\mu_2 | s_1, s_2)^{t_1} \mathbf{S}_{21}(\mathbf{q}^2 \mu_2/\mu_1 | -(s_2 \mathbf{q})^{-1}, -(s_1 \mathbf{q})^{-1})^{t_2} \simeq \mathbf{I}, \quad (2.19)$$

which will be used later on.

Below, it will be convenient to use a slightly different set of spectral variables. Namely for the  $\mathbf{L}$ -operator

$$\mathbf{L}(\mu | s) = \mathcal{L}(x, x', y), \quad \mu = \xi x x' / y^2, \quad s = x / (x' \xi), \quad \xi = i\sqrt{\mathbf{q}}, \quad (2.20)$$

we will use new spectral variables  $x, x'$  and  $y$ . Explicitly, using the formulae (2.4), (2.6) and (2.7), one obtains

$$\left( \mathcal{L}(x, x'/\xi, y) \right)_a^{a'} = \begin{pmatrix} \frac{x x'}{y^2} \delta_{a, a'+1} - \frac{y^2}{x x'} \delta_{a, a'-1} & \mathbf{q}^a \left( \frac{x}{x'} \delta_{a, a'+1} - \frac{x'}{x} \delta_{a, a'-1} \right) \\ \mathbf{q}^{-a} \left( \frac{x}{x'} \delta_{a, a'-1} - \frac{x'}{x} \delta_{a, a'+1} \right) & \frac{x x'}{y^2} \delta_{a, a'-1} - \frac{y^2}{x x'} \delta_{a, a'+1} \end{pmatrix}, \quad (2.21)$$

where the indices  $a, a' \in \mathbb{Z}$  refer to the quantum space. Next, let us parameterize the matrix elements of the operator  $\mathbf{S}_{12}(\mu_1/\mu_2 | s_1, s_2)$  entering (2.11),

$$\mathbf{S}_{12}(\mu_1/\mu_2 | s_1, s_2)_{a,b}^{a',b'} = \mathcal{S}(x, x', y, y')_{a,b}^{a',b'}, \quad (2.22)$$

by a new set of spectral variables

$$\mu_1/\mu_2 = xx'/(yy'), \quad s_1 = x/(x'\xi), \quad s_2 = y/(y'\xi). \quad (2.23)$$

Here the matrix indices  $a, a'$  refer to the space  $\pi_{s_1}$  and the indices  $b, b'$  to the space  $\pi_{s_2}$ . With these definitions one can bring the YBE (2.11) to the form

$$\begin{aligned} & \sum_{a', b' \in \mathbb{Z}} \mathcal{L}(x, x', z)_a^{a'} \mathcal{L}(y, y', z)_b^{b'} \mathcal{S}(x, x', y, y')_{a', b'}^{a'', b''} \\ &= \sum_{a', b' \in \mathbb{Z}} \mathcal{S}(x, x', y, y')_{a, b}^{a', b'} \mathcal{L}(y, y', z)_{b'}^{b''} \mathcal{L}(x, x', z)_{a'}^{a''}. \end{aligned} \quad (2.24)$$

where  $a, a'', b, b'' \in \mathbb{Z}$ . Note, that there are no infinite summations: each sum above contains exactly four terms, due to the special form (2.21) of the  $\mathbf{L}$ -operators.

Finally, with the new notations the inversion relation (2.13) and (2.19) read

$$\sum_{a', b' \in \mathbb{Z}} \mathcal{S}(x, x', y, y')_{a, b}^{a', b'} \mathcal{S}(y, y', x, x')_{b', a'}^{b'', a''} \simeq \delta_{a, a''} \delta_{b, b''} \quad (2.25)$$

$$\sum_{a', b' \in \mathbb{Z}} \mathcal{S}(x, x', y, y')_{a', b}^{a, b'} \mathcal{S}(\xi y', \xi y, x'/\xi, x/\xi)_{b', a'}^{b'', a''} \simeq \delta_{a, a''} \delta_{b, b''}, \quad (2.26)$$

where the symbol  $\simeq$  means the proportionality up to a scalar factor independent of spins.

### 3 From vertex models to Ising-type models

#### 3.1 Face-vertex correspondence

In this section we solve the YBE (2.24) together with the inversion relations (2.25), (2.26) and find an explicit expression for the operator  $\mathcal{S}(x, x', y, y')$  (the notation introduced in (2.22)). The calculations are based on the idea of factorized  $R$ -matrices, the Baxter's "propagation through the vertex" techniques and the "face-vertex" correspondence [1]. Note, in particular, that this scheme was successfully used in [28].

The  $\mathbf{L}$ -operator of the type (2.8) (but for cyclic representations of the Weyl algebra (2.7) with  $\mathbf{q}$  being a root of unity) has previously appeared in [23] in the context of the chiral Potts model [7–9]. The results of [23] suggest that the matrix elements  $\mathcal{S}(x, x', y, y')_{a, b}^{a', b'}$ , solving (2.24), factorize into a product of four factors depending on two spins only. Indeed, we will show that

$$\mathcal{S}(x, x', y, y')_{a, b}^{a', b'} = W_{x'/y}(a - b) W_{x/y}(b' - a') \overline{W}_{x/y}(a - b') \overline{W}_{x'/y'}(b - a') \quad (3.1)$$

where the functions  $W_{x/y}(a - b)$  and  $\overline{W}_{x/y}(a - b)$  depend on the ratio  $x/y$  of two spectral variables and on the difference  $(a - b)$  of two spins.<sup>3</sup> It is well known, that the matrix elements  $\mathcal{S}(x, x', y, y')_{a, b}^{a', b'}$  can be used as Boltzmann weights to define a vertex model on the square lattice. The factorization (3.1) implies that this model can be reformulated as an Ising-type model with only two-spin interaction through the edges of the (medial) lattice.

Our considerations split into two steps. First we show that the factorization (3.1) is a corollary of two rather simple (Yang-Baxter type) "exchange relations", involving only the two-spin weights  $W$  and  $\overline{W}$  and some explicitly known tri-spin weights. Then we solve all these relations and explicitly determine the unknown two-spin weights  $W$  and  $\overline{W}$ .

---

<sup>3</sup>Initially, one could assume that all four functions in the RHS of (3.1) are different, but the a simple analysis (which we skip here) shows that they should pairwise coincide. The  $R$ -matrix factorization of the type (3.1) usually take place when the Cartan element  $K$  of of the algebra (2.5) is realized as the shift operator (see, e.g., [28] or Sect.5 of ref. [29]).

The proof of (3.1) is based on important factorization properties of the  $\mathbf{L}$ -operator (2.21), which we describe below. Introduce an infinite set of two-dimensional vectors labelled by  $a, a' \in \mathbb{Z}$

$$\begin{aligned}\Phi(x, y)_{a, \sigma}^{a'} &= (i q^{\frac{\sigma}{2}} x/y)^\sigma \delta_{a, a'+1} + (-i q^{\frac{\sigma}{2}} y/x)^\sigma \delta_{a, a'-1}, \\ \bar{\Phi}(x, y)_{a, \sigma}^{a'} &= -i (q^{-\frac{\sigma}{2}} x/y)^\sigma \delta_{a, a'+1} - i (q^{-\frac{\sigma}{2}} y/x)^\sigma \delta_{a, a'-1},\end{aligned}\tag{3.2}$$

with the components indexed by  $\sigma = \pm 1$ . The half-integer powers of  $q$  here and in some of the equations below are understood as  $q^{\frac{\sigma}{2}} = (\sqrt{q})^\sigma$ , where the sign of the square root should be chosen consistently throughout all equation. The above vectors satisfy important orthogonality relations

$$\sum_{a' \in \mathbb{Z}} \Phi(x, y)_{a, \sigma}^{a'} \bar{\Phi}(x, y)_{a, \sigma'}^{a'} = [x^2/y^2] \delta_{\sigma, \sigma'}, \quad \sum_{\sigma = \pm 1} \bar{\Phi}(x, y)_{a, \sigma}^{a'} \Phi(x, y)_{a, \sigma}^{a''} = [x^2/y^2] \delta_{a', a''}.\tag{3.3}$$

where we used the notation  $[x] = x - x^{-1}$ . It is convenient to also introduce another set of two-dimensional vectors

$$\Omega(x, y)_{a, \sigma}^{a'} = \Phi(x/\xi, y)_{a, \sigma}^{a'}, \quad \bar{\Omega}(x, y)_{a, \sigma}^{a'} = \bar{\Phi}(\xi x, y)_{a, \sigma}^{a'},\tag{3.4}$$

which satisfy slightly different orthogonality conditions

$$\sum_{a \in \mathbb{Z}} \Omega(x, y)_{a, \sigma}^{a'} \bar{\Omega}(x, y)_{a, \sigma'}^{a'} = [x^2/y^2] \delta_{\sigma, \sigma'}, \quad \sum_{\sigma = \pm 1} \bar{\Omega}(x, y)_{a, \sigma}^{a'} \Omega(x, y)_{a, \sigma}^{a''} = [x^2/y^2] \delta_{a', a''}.\tag{3.5}$$

where  $\sigma, \sigma' = \pm 1$ . Using the explicit form of the two-by-two  $L$ -operator (2.21) it is easy to check that

$$(\mathcal{L}(x, x', z)_a^{a'})_{i, i'} = \Phi(x, z)_{a, i}^{a'} \bar{\Omega}(x', z)_{a, i'}^{a'} = \begin{array}{c} \begin{array}{c} \uparrow \\ a' \\ \uparrow \\ \Phi \\ \downarrow \\ a \\ \downarrow \\ x' \end{array} \begin{array}{c} z \\ \rightarrow \\ z \\ \rightarrow \\ z \\ \rightarrow \\ i' \end{array} \end{array}\tag{3.6}$$

Note, that the indices  $(i, i') = (+, +)$  refer to the top left element in (2.21). Here we have used the following graphical notations

$$\Phi(x, z)_{a, i}^{a'} = \begin{array}{c} \begin{array}{c} x \\ \swarrow \\ a' \\ \swarrow \\ z \\ \swarrow \\ i \end{array} \begin{array}{c} \swarrow \\ a \\ \swarrow \\ z \\ \swarrow \\ i \end{array} \end{array} \quad \Omega(x, z)_{a, i}^{a'} = \begin{array}{c} \begin{array}{c} x \\ \swarrow \\ a \\ \swarrow \\ z \\ \swarrow \\ i \end{array} \begin{array}{c} \swarrow \\ a' \\ \swarrow \\ z \\ \swarrow \\ i \end{array} \end{array}\tag{3.7}$$

and

$$\bar{\Phi}(x, z)_{a, i}^{a'} = \begin{array}{c} \begin{array}{c} i \\ \swarrow \\ z \\ \swarrow \\ a' \end{array} \begin{array}{c} x \\ \swarrow \\ a \\ \swarrow \\ z \\ \swarrow \\ i \end{array} \end{array} \quad \bar{\Omega}(x, z)_{a, i}^{a'} = \begin{array}{c} \begin{array}{c} x \\ \swarrow \\ a' \\ \swarrow \\ z \\ \swarrow \\ i \end{array} \begin{array}{c} \swarrow \\ a \\ \swarrow \\ z \\ \swarrow \\ i \end{array} \end{array}\tag{3.8}$$

There are two types of spin variables in these pictures. The variables  $a, a' \in \mathbb{Z}$  are the “face spins” assigned to the shaded faces, while  $i, i' = \pm 1$  are the edge spins (same as in the 6-vertex models) assigned to the directed solid lines in the unshaded areas. Moreover these lines (as well as their

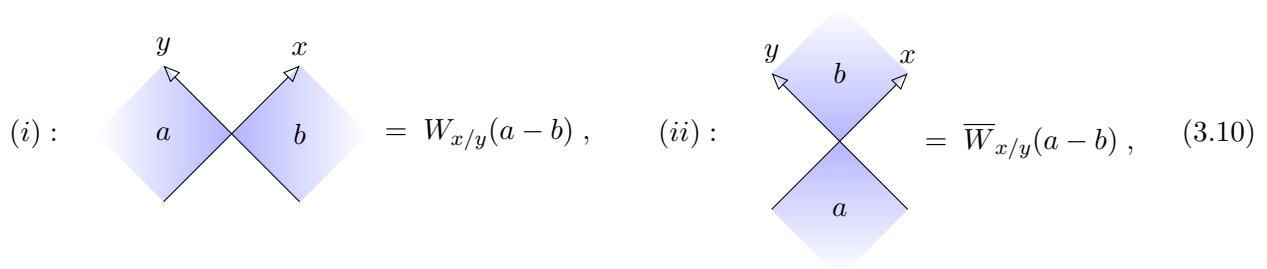


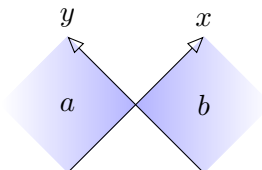
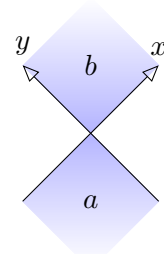
dashed continuations into shaded areas) carry a spectral variable  $z$ . Another spectral parameter  $x$  is assigned to the directed thin lines, which separate the shaded and unshaded areas.

After these preparations, let us now substitute (3.1) and (3.6) into the YBE (2.24). The latter then reduces to two rather simple exchange relations involving the two-spin weights  $W_x(a-b)$  and  $\bar{W}_x(a-b)$  and the “face-vertex” vectors  $\Phi$  and  $\bar{\Omega}$ , defined in (3.2) and (3.4), which can be viewed as tri-spin weights. The first of these relations reads

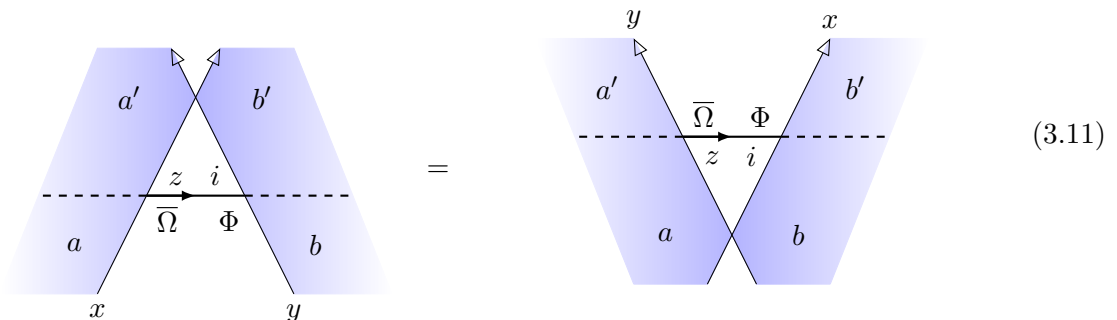
$$W_{x/y}(a'-b') \sum_i \bar{\Omega}(x, z)_{a,i}^{a'} \Phi(y, z)_{b,i}^{b'} = W_{x/y}(a-b) \sum_i \bar{\Omega}(y, z)_{a,i}^{a'} \Phi(x, z)_{b,i}^{b'}, \quad (3.9)$$

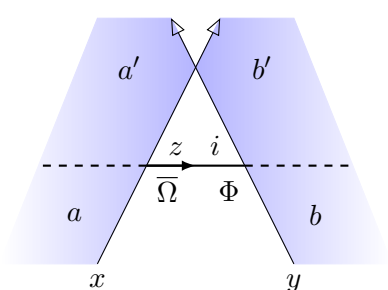
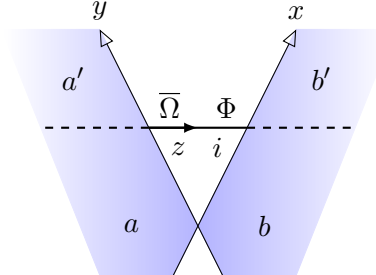
where  $a, a', b, b' \in \mathbb{Z}$  (note, there is no summation over these indices). Introduce the following graphical notations for the two-spin weights,



(i) :  =  $W_{x/y}(a-b)$ ,      (ii) :  =  $\bar{W}_{x/y}(a-b)$ ,      (3.10)

by associating them with intersections of thin lines separating the shaded and unshaded areas. Note that there are two types of such intersections distinguished by the orientation of the thin lines with respect to the shaded faces. With these notations one can represent (3.9) as



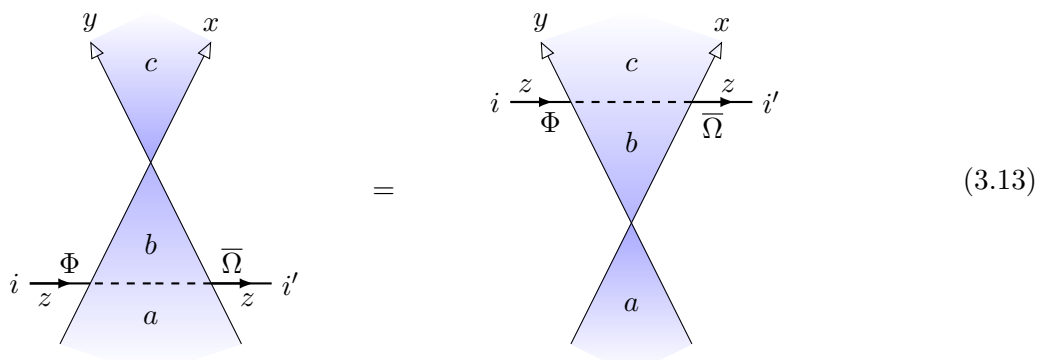
 =       (3.11)

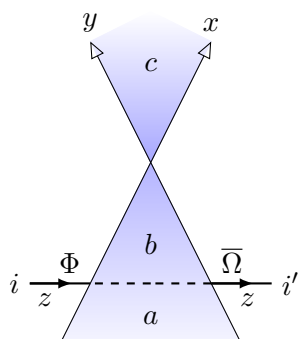
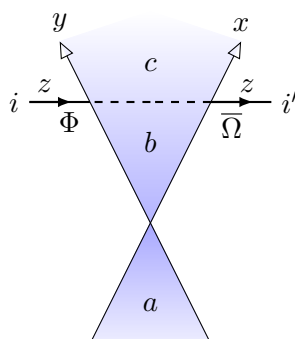
where the summation is taken over the edge spins  $i$  assigned to the “internal” (bounded) directed solid lines.

The second exchange relation (arizing upon the substitution of (3.1) and (3.6) into the YBE (2.24)) reads

$$\sum_b \Phi(x, z)_{a,i}^b \bar{\Omega}(y, z)_{a,i'}^b \bar{W}_{x/y}(b-c) = \sum_b \bar{W}_{x/y}(a-b) \Phi(y, z)_{b,i}^c \bar{\Omega}(x, z)_{b,i'}^c. \quad (3.12)$$

It can be represented graphically as



 =       (3.13)

where the summation over the spins  $b$ , assigned to the “interior” (bounded) faces, is assumed. The boundary spins  $a, c$  on the “exterior” (unbounded) faces, as well the edge spins  $i, i'$  on the external edges are fixed. Finally, with the same graphical notations the YBE (2.24) is represented as in Fig.1.

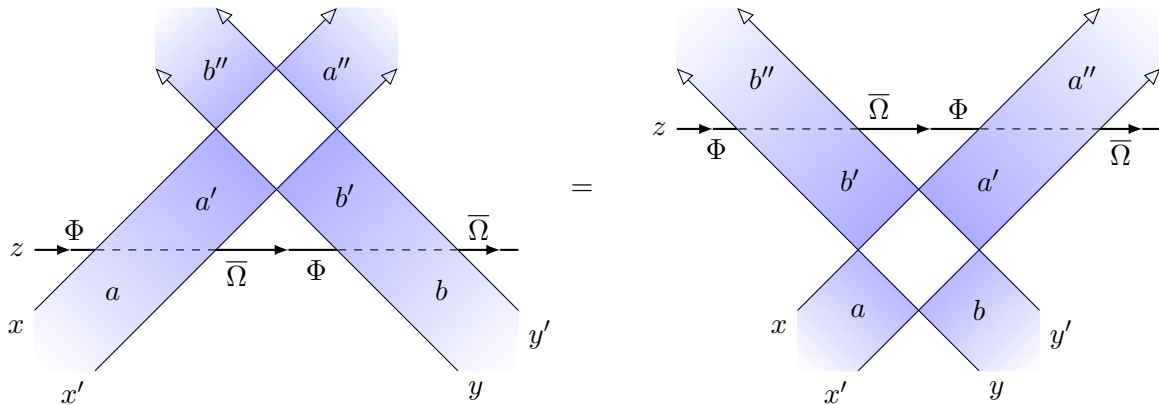


**Figure 1:** A graphical representation of the Yang-Baxter equation (2.24).

It is fairly simple to verify that the relations (3.12) and (3.9) imply eq.(2.24). First, substitute (3.1) and (3.6) into (2.24). Then, using (i) the relation (3.9), (ii) the relation (3.12) (twice) and, finally, (iii) the relation (3.9) again, one can easily transform one side of (2.24) into the other. To visualize this calculation consider the diagram on the left side Fig. 1. Now, let us move the horizontal  $z$ -line upwards, through the intersection points of the other lines, and then consecutively use an appropriate relation (3.9) or (3.12) at each crossing transition. In this way the left diagram in Fig. 1 is transformed to the right one, thereby proving (2.24).

### 3.2 Calculation of the two-spin weights

Thus, we have shown that the YBE (2.24) with the factorized matrix  $\mathcal{S}$ , given by (3.1), is a corollary of the Yang-Baxter type exchange relations (3.9) and (3.12). The next step is to solve these relations together with the inversion relations (2.25) and (2.26) to find the two-spin weights  $W_x(a-b)$  and  $\bar{W}_x(a-b)$ . The corresponding calculations are presented in the Appendix A. We show that, to within overall normalization factors and some trivial equivalence transformations<sup>4</sup>, the above relations uniquely determine the two-spin weights

$$W_x(n) = x^n \frac{(-q^{1+n} x^2; q^2)_\infty}{(-q^{1+n}/x^2; q^2)_\infty}, \quad \bar{W}_x(n) = W_{\xi/x}(n) = \left(\frac{\xi}{x}\right)^n \frac{(q^{2+n}/x^2; q^2)_\infty}{(q^n x^2; q^2)_\infty}, \quad (3.14)$$

where  $\xi = i\sqrt{q}$  and  $(x; q^2)_\infty$  denotes the  $q$ -Pochhammer symbol

$$(x; q^2)_\infty = \prod_{k=0}^{\infty} (1 - x q^{2k}). \quad (3.15)$$

Below we will use the notations

$$\sigma(x) = \frac{(-q/x; q)_\infty}{(x; q)_\infty}, \quad \kappa_s = \frac{(q; q)_\infty}{(-q; q)_\infty}. \quad (3.16)$$

The weights (3.14) possess the following important properties:

<sup>4</sup>All the equations (3.9), (3.12) and (2.25), (2.26) (with  $\mathcal{S}$  given by (3.1)) are invariant w.r.t a simple transformation  $\bar{W}_x(n) \rightarrow (-1)^n \bar{W}_x(n)$  (and, similarly, for  $W$ ). Our choice of these signs is governed by the positivity requirements, see the paragraph containing (3.17).

(i) *Positivity*

If the parameter  $\xi = i\sqrt{q}$  and the spectral variable  $x$  are real and belong to the domain

$$0 < \xi < x < 1, \quad (3.17)$$

then the weights (3.14) are *real and positive*.

(ii) *Reflection and crossing symmetry*

$$W_x(n) = W_x(-n), \quad \overline{W}_x(n) = \overline{W}_x(-n), \quad \overline{W}_x(n) = W_{\xi/x}(n), \quad (3.18)$$

(iii) *Second order recurrence relations*

$$\frac{\overline{W}_x(n)}{\overline{W}_x(n-2)} = -\frac{q - q^{n-1}x^2}{x^2 - q^n}, \quad \frac{W_x(n)}{W_x(n-2)} = \frac{x^2 + q^{n-1}}{1 + q^{n-1}x^2}, \quad n \in \mathbb{Z}, \quad (3.19)$$

(iv) *Inversion relations*

$$\sum_{n \in \mathbb{Z}} \overline{W}_x(a-n) \overline{W}_{1/x}(n-b) = \Upsilon(x) \delta_{a,b}, \quad W_x(n) W_{1/x}(n) = 1. \quad (3.20)$$

where

$$\Upsilon(x) = \kappa_s^2 \sigma(x^2) \sigma(x^{-2}), \quad (3.21)$$

with  $\sigma(x)$  and  $\kappa_s$  defined in (3.16). Using the crossing symmetry (3.18) these relations can also be rewritten as

$$\sum_{n \in \mathbb{Z}} W_{\xi/x}(a-n) W_{\xi x}(n-b) = \Upsilon(x) \delta_{a,b}, \quad \overline{W}_{\xi/x}(n) \overline{W}_{\xi x}(n) = 1. \quad (3.22)$$

(v) *Star-triangle relation*

The weights (3.14) satisfy the star-triangle relation of the form,

$$\begin{aligned} \sum_{d \in \mathbb{Z}} \overline{W}_{y/z}(a-d) W_{x/z}(b-d) \overline{W}_{x/y}(d-c) \\ = \mathcal{R} W_{x/y}(b-a) \overline{W}_{x/z}(a-c) W_{y/z}(b-c), \end{aligned} \quad (3.23)$$

where  $\mathcal{R}$  is the scalar factor

$$\mathcal{R} = \kappa_s \frac{\sigma(y^2/z^2) \sigma(x^2/y^2)}{\sigma(x^2/z^2)}, \quad (3.24)$$

and the function  $\sigma(x)$  and the constant  $\kappa_s$  are defined in (3.16). Note that  $\kappa_s$  is the ‘‘rapidity-independent factor’’ of the star-triangle relation [11], which does not depend on the normalization of the weights  $W$  and  $\overline{W}$ , obeying the crossing symmetry (3.18).

Using the graphical notations (3.10) one can represent the inversion relations (3.20) as in Fig.2. Similarly, the star-triangle relation (3.23) is presented in Fig.3. Recall, that in these figures the spins are assigned to the shaded faces, the summation over the interior spins is assumed and the boundary spins are kept fixed. The proof of these relations is given below. Here we just remark that the properties (iii), (iv), listed above, ensure the fulfillment of all defining relations for the weights (3.14). Indeed, using the explicit form of the face-vertex vectors (3.2) and (3.4) one can simply rewrite the exchange relations (3.9), (3.12) as the recurrence relations (3.19). Next, the inversion relations (2.25) and (2.26) simply follow from the (3.1), (3.20) and (3.22).

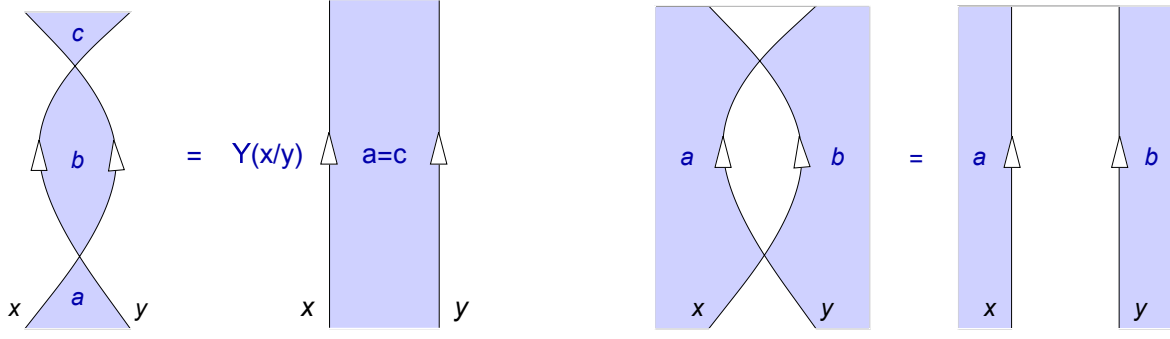


**Figure 2:** Graphical representation of the first and second inversion relations in (3.20) (on the left and right sides of the picture, respectively), using the graphical notations (3.10) for the Boltzmann weights.

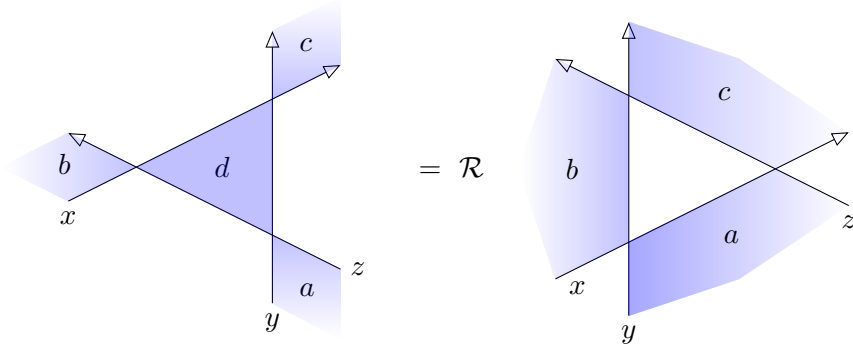


**Figure 3:** Graphical representation of the star-triangle relation (3.23).

### 3.3 Duality transformation

Since the two-spin weights only depend on the spin difference, it is natural to consider their Fourier transformation

$$\bar{\omega}_x(\varphi) = \kappa_s^{-1} \sigma(x^2) \sum_{n \in \mathbb{Z}} e^{i\varphi n} W_x(n), \quad \omega_x(\varphi) = \kappa_s^{-1} \sigma(x^2)^{-1} \sum_{n \in \mathbb{Z}} e^{i\varphi n} \bar{W}_x(n), \quad (3.25)$$

with real  $0 \leq \phi < 2\pi$ . From (3.18) it follows that

$$\omega_x(\varphi) = \omega_x(-\varphi), \quad \bar{\omega}_x(\varphi) = \bar{\omega}_x(-\varphi), \quad \bar{\omega}_x(\varphi) = \omega_{\xi/x}(\varphi). \quad (3.26)$$

Explicitly, one obtains

$$\begin{aligned} \bar{\omega}_x(\varphi) &= \sigma(xe^{i\phi}) \sigma(xe^{-i\phi}) = \frac{(-qx^{-1}e^{i\varphi}, -qx^{-1}e^{-i\varphi}; q)_\infty}{(xe^{i\varphi}, xe^{-i\varphi}; q)_\infty}, \\ \omega_x(\varphi) &= \sigma(\xi x^{-1}e^{i\phi}) \sigma(\xi x^{-1}e^{-i\phi}) = \frac{(\xi x e^{i\varphi}, \xi x e^{-i\varphi}; q)_\infty}{(\xi x^{-1}e^{i\varphi}, \xi x^{-1}e^{-i\varphi}; q)_\infty}. \end{aligned} \quad (3.27)$$

The derivation is based on an extension of the Ramanujan  ${}_1\psi_1$  bilateral summation formula [26],

$$\sum_{n \in \mathbb{Z}} \frac{(bq^n; q^2)_\infty}{(aq^n; q^2)_\infty} z^n = \frac{(q; q)_\infty}{(-q; q)_\infty} \frac{(b/a; q^2)_\infty}{(b/az^2; q^2)_\infty} \frac{(-q/z; q)_\infty}{(z; q)_\infty} \frac{(az, q/az; q)_\infty}{(a, q/a; q)_\infty} \quad (3.28)$$

valid for  $\sqrt{|b/a|} < z < 1$ .

Using (3.25) and (3.27) it is easy to prove the first relation in (3.20) (the second one there is obvious) and also derive the inversion relations for the  $\omega$ -weights,

$$\frac{1}{(2\pi)^2} \int_{-\pi}^{\pi} d\varphi \overline{\omega}_x(\alpha - \varphi) \overline{\omega}_{1/x}(\varphi - \beta) = \kappa_s^{-2} \sigma(x^2) \sigma(x^{-2}) \delta(\alpha - \beta), \quad \omega_x(\varphi) \omega_{1/x}(\varphi) = 1. \quad (3.29)$$

Finally, equivalently rewriting the star-triangle relation (3.23) in terms of the  $\omega$ -weights (3.25), one obtains

$$\begin{aligned} \int_{-\pi}^{\pi} \frac{d\varphi}{2\pi} \overline{\omega}_{y/z}(\alpha - \varphi) \omega_{x/z}(\beta - \varphi) \overline{\omega}_{x/y}(\varphi - \gamma) \\ = \tilde{\mathcal{R}} \omega_{x/y}(\beta - \alpha) \overline{\omega}_{x/z}(\alpha - \gamma) \omega_{y/z}(\beta - \gamma), \end{aligned} \quad (3.30)$$

where

$$\tilde{\mathcal{R}} = \kappa_s^{-1} \frac{\sigma(y^2/z^2) \sigma(x^2/y^2)}{\sigma(x^2/z^2)}. \quad (3.31)$$

Using now the explicit expressions (3.27) one can easily transform (3.30) into the concise integral identity (1.11), presented in the Introduction. As remarked before this identity can be derived from the “*constant beta pentagon equation*”, obtained by Garoufalidis and Kashaev [27] (see eq.(47) therein). Mathematically, the derivation is not very difficult, so we leave it as an exercise for the reader. However, from a conceptual point of view it is very interesting that the *pentagon equation* of [27] (which has a specific structure of the “five term quantum dilogarithm identity” [30] or the “restricted star-triangle relation” of [31]) can be reinterpreted as the full star-triangle relation (3.30).

To summarize, the proof of the inversion relations (3.20), (3.29) is based on the summation formula (3.28); the star-triangle relations (3.23), (3.30) and (1.11) can be derived from the result of [27]. In addition, we have thoroughly verified all key equations numerically.

## 4 An integrable model on general planar graphs

### 4.1 “Z-invariant” lattice models

A solvable edge-interaction model on rather general planar graphs can be defined in the following way [32, 33]. Consider a finite set of  $L$  directed lines forming a graph  $\mathcal{L}$  of the type shown in Fig. 4. The lines (in this case six) head generally from the bottom of the graph to the top, intersecting one another on the way. Let  $V(\mathcal{L})$  denote the set of vertices of  $\mathcal{L}$  formed by these intersections. The lines can go locally downwards, but there can be no closed directed paths in  $\mathcal{L}$ . This means that one can always distort  $\mathcal{L}$ , without changing its topology, so that the lines always head upwards.

To each line  $\ell$  of  $\mathcal{L}$  associate its own spectral variable  $x_\ell$ , taking positive real values. Next, shade alternative faces of  $\mathcal{L}$  as shown in Fig. 4 and place integer valued spins  $a_i \in \mathbb{Z}$  on all shaded faces. Among those we will sometimes distinguish the interior (bounded) and exterior (unbounded) faces. The spins  $a_i$  and  $a_j$  interact only if the corresponding faces  $i$  and  $j$  have a common vertex  $(i, j)$ . There are two types of vertices distinguished by the orientation of the lines passing through the vertex relative to the shaded faces. They are shown in (3.10) on the left (first type) and on the right (second type) sides of the picture. It is convenient to introduce a “spectral parameter ratio variable”

$$s = \begin{cases} x/y, & \text{for a first type vertex,} \\ (\xi y)/x, & \text{for a second type vertex,} \end{cases} \quad (4.1)$$

where the variables  $x$  and  $y$  are arranged exactly as in (3.10). Then, each vertex  $(i, j)$  is assigned with the Boltzmann weight  $\rho(s_{ij}) W_{s_{ij}}(a_i - a_j)$ , where  $a_i$  and  $a_j$  are the spins on the shaded faces across the vertex,  $s_{ij}$  is the corresponding ratio variable (4.1) and  $\rho(s_{ij})$  is the normalization factor. The partition function is defined as a sum over all configurations of interior spins with the weight equal to the product of the local weights over all vertices of  $\mathcal{L}$ ,

$$Z = \sum_{\substack{\text{interior} \\ \text{spins}}} \prod_{(i,j) \in V(\mathcal{L})} \rho(s_{ij}) W_{s_{ij}}(a_i - a_j). \quad (4.2)$$

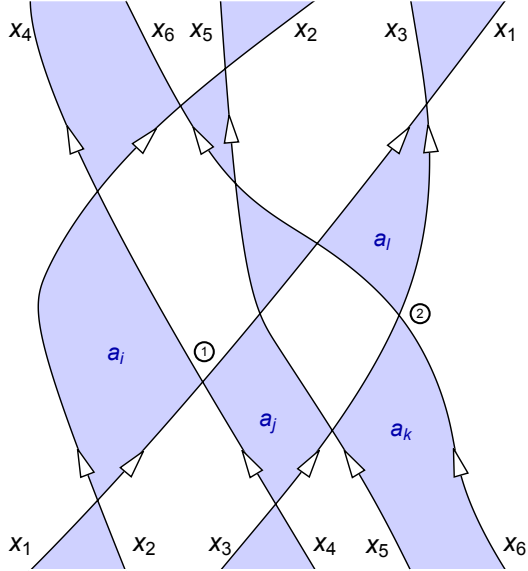


**Figure 4:** The graph  $\mathcal{L}$  formed by directed thin lines and alternatively shaded faces. The lines of  $\mathcal{L}$  are assigned with the spectral variables  $x_1, x_2, x_3, \dots$ . The symbols ① and ② mark generic examples of the first and second type vertices, respectively, as defined in (3.10).

The spins on exterior faces are kept fixed. It is worth noting, that, more conventionally, the above model can be viewed as an edge interaction model on the irregular planar graph  $\mathcal{G}$ , shown in Fig. 5 with bold lines and filled circles. The sites of  $\mathcal{G}$  are identified with the (shaded) faces of the original graph  $\mathcal{L}$ , while its edges are identified with the vertices of  $\mathcal{L}$ , so that the set of edges of the new graph  $\mathcal{G}$  coincides with set of vertices of the original graph  $\mathcal{L}$ , i.e.,  $E(\mathcal{G}) \equiv V(\mathcal{L})$ . With this correspondence

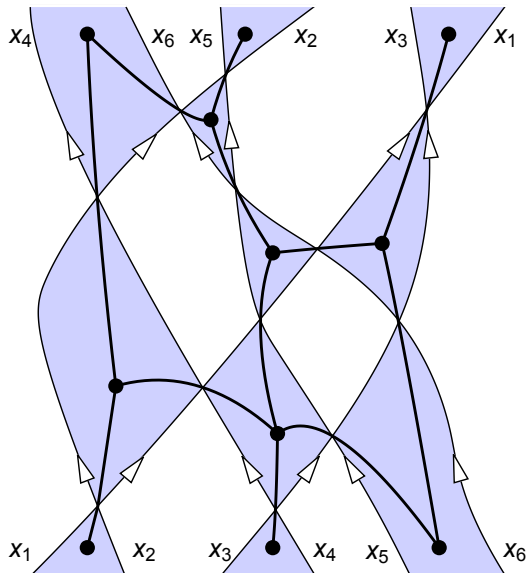


**Figure 5:** The graph  $\mathcal{G}$ , whose sites (shown by filled circles) are identified with the shaded faces of  $\mathcal{L}$ , and the edges (shown by bold lines) are identified with the vertices of  $\mathcal{L}$ .

the original graph  $\mathcal{L}$  is the *medial* graph of  $\mathcal{G}$ . Actually, we could have started with the planar graph  $\mathcal{G}$  and then constructed  $\mathcal{L}$  as the medial graph. For instance, taking into account the crossing symmetry (3.18), one could easily see that the expression (1.9) is just a particular case of (4.2) when the graph  $\mathcal{G}$  is a homogeneous square lattice.

The partition function (4.2) possesses remarkable invariance properties. It remains unchanged (up

to simple  $\rho(s_{ij})$ ,  $\sigma(s_{ij}^{\pm 2})$  and  $\kappa_s$  factors) by continuously deforming the lines of  $\mathcal{L}$  with their boundary positions kept fixed, as long as the graph  $\mathcal{L}$  remains directed. In particular, no closed directed paths are allowed to appear<sup>5</sup>. It is easy to see that all such transformations reduce to a combination of the moves shown in Fig. 3 and Fig. 2, corresponding to the star-triangle (3.23) and inversion relations (3.20). Given that the graphs  $\mathcal{L}$  and  $\mathcal{G}$  can undergo rather drastic changes, the above invariance statement (called the “Z-invariance” [32]) is rather non-trivial. In particular, it leads to important factorization properties of the partition function in the large lattice limit. Consider a generic planar graph  $\mathcal{G}$  with a large number of sites,  $M$ , a large number of edges of the order of  $\sim 2M$  and the number of boundary sites of the order of  $O(M^{1/2})$ . Assume that the boundary spins are kept fixed. Then, following [32], one can show that the leading asymptotics of the partition function (4.2) at large  $M$  has the form [32, 37]

$$\log Z = M \log \kappa_s + \sum_{(ij) \in E(\mathcal{G})} \log \kappa_e(s_{ij}) + O(\sqrt{M}), \quad (4.3)$$

where  $\kappa_e(x)$  is the single-edge contribution and  $\kappa_s$  is the single-site contribution to the partition function in the thermodynamic limit. Note that the factor  $\kappa_s$ , defined in (3.16), is the “rapidity-independent factor” [11] for the star-triangle relation (3.23). Remarkably, the factors  $\kappa_s$  and  $\kappa_e(x)$  are universal; they are independent of the graph  $\mathcal{G}$ .

Note, that the original formulation of the Z-invariant models [32] involved lattices  $\mathcal{L}$  formed by arbitrary intersections of straight lines. Here we follow a generalized formulation [33] where the straight lines are replaced by arbitrary curved lines, as it was described above.

## 4.2 Inversion relations

In the large-lattice limit the partition function (4.2) can be calculated using the inversion relation method [34–36]. For example, for a regular square lattice of  $M$  sites there are only two different spectral parameters  $x$  and  $y$ . Correspondingly, a half of edges will have the ratio variable (4.1) equal to  $x/y$ , while the other half will have it equal to  $(\xi y)/x$ . Let

$$\kappa^{(\text{sq})}(x/y) = Z^{1/M}, \quad M \rightarrow \infty, \quad (4.4)$$

be the partition function per site in the large lattice limit, where the superscript “(sq)” stands for “square lattice”. Then, using the symmetry, inversion and star-triangle relations (3.18), (3.20), (3.23) one can show that [34–36],

$$\kappa^{(\text{sq})}(x) \kappa^{(\text{sq})}(x^{-1}) = \kappa_s^2 \rho(x) \rho(x^{-1}) \rho(\xi x) \rho(\xi x^{-1}) \sigma(x^2) \sigma(x^{-2}), \quad (4.5)$$

$$\kappa^{(\text{sq})}(x) = \kappa^{(\text{sq})}(\xi/x). \quad (4.6)$$

Together with an appropriate analyticity assumptions the above inversion and symmetry relations uniquely determine  $\kappa^{(\text{sq})}(x)$  (see (5.9) below).

For the Ising-type models these relations could be further refined. First, comparing (4.4) with (4.3) one concludes

$$\kappa^{(\text{sq})}(x) = \kappa_s \kappa_e(x) \kappa_e(\xi/x). \quad (4.7)$$

Indeed, there are exactly two edges (one of each type) for each site of a regular square lattice. Correspondingly, the partition function per site (4.7) is a product of the spectral parameter independent single-site factor  $\kappa_s$  and two single-edge factors  $\kappa_e(x)$  and  $\kappa_e(\xi/x)$ .

Next, consider the star-triangle relation (3.23). It is easy to see that the factor  $\mathcal{R}$  there can be absorbed into a rescaling of the weights  $\bar{W}$  and to a redefinition of the sum over the interior spin in the LHS of (3.23),

$$\bar{W}_x(n) \rightarrow \frac{1}{\sigma(x^2)} \bar{W}_x(n) \quad \sum_{d \in \mathbb{Z}} \rightarrow \frac{1}{\kappa_s} \sum_{d \in \mathbb{Z}} \quad (4.8)$$

<sup>5</sup>Actually, these restrictions can be removed if one properly defines “reflected” spectral variables for downward going lines, see Sect.3 of [33] for further details.

Now consider the effect of a star-triangle move (from the triangle to star) in the expression (4.3). Such a move exchanges the edges of the first type with edges of the second type (and vice versa). For instance, the first type edge with the weight  $W_{x/y}(n)$  is replaced by the second type edge with the (rescaled) weight  $\bar{W}_{x/y}(n)/\sigma(x^2/y^2)$ . Taking into account the crossing symmetry (3.18) between the weights  $W$  and  $\bar{W}$ , the normalization factors  $\rho(s_{ij})$  in the definition (4.2) and the fact that the partition function (4.3) does not change under the star-triangular move, one obtains [18, 37]

$$\frac{\kappa_e(\xi/x)}{\rho(\xi/x)} = \sigma(x^2) \frac{\kappa_e(x)}{\rho(x)}. \quad (4.9)$$

Next, the inversion relation moves (3.20), shown in Fig. 2, trivially lead to

$$\kappa_e(\xi x) \kappa_e(\xi/x) = \rho(\xi x) \rho(\xi x^{-1}) \sigma(x^2) \sigma(x^{-2}), \quad \kappa_e(x) \kappa_e(x^{-1}) = \rho(x) \rho(x^{-1}), \quad (4.10)$$

where the normalization factors in (4.3) have been taken into account. Note, that the relation (4.9) combined with the first relation in (4.10) imply the second relation there. Finally, it is easy to see that the above relations together with (4.7) immediately imply (4.6).

### 4.3 Factorization of the partition function

The partition function (4.2) depends on the exterior spins and the spectral variables  $x_1, x_2, \dots, x_L$ . Of course, it also depends on the graph  $\mathcal{L}$ , but only on a relative ordering (permutation) of the rapidity lines at the boundaries and not on their arrangement inside the graph. Naturally, this graph can be identified with an element of the permutation group. Then the partition function  $Z$  can be regarded as the permutation group representation matrix, acting non-trivially on the spins at the lower and upper boundaries. In particular, if the associated permutation factorizes into a product of two permutations, where the first one only acts on the first  $K$  spectral variables  $x_1, x_2, \dots, x_K$ , while the second one acts on the remaining variables  $x_{K+1}, \dots, x_L$ , then using the  $Z$ -invariance the graph  $\mathcal{L}$  can be transformed into two disjoint graphs. Correspondingly, the partition function factorizes (up to simple  $\rho(s_{ij})$ ,  $\sigma(s_{ij}^{\pm 2})$  and  $\kappa_s$  factors) into the product of two partition functions, associated with these two graphs.

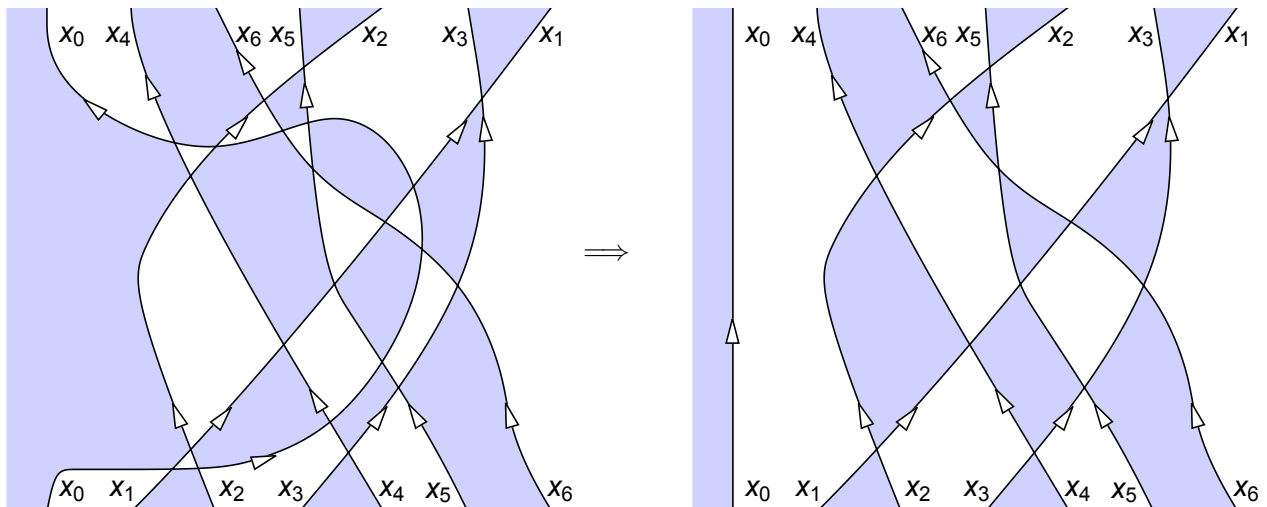


**Figure 6:** Using the star-triangle and inversion relation moves the line  $x_0$  can be disentangled from the rest of the graph  $\mathcal{L}$ . Therefore, the partition functions corresponding to the above two graphs coincide up to the simple  $\rho(s_{ij})$ ,  $\sigma(s_{ij}^{\pm 2})$  and  $\kappa_s$  factors, associated with the elementary moves.

As an illustration of such factorization consider the graphs shown in Fig. 6. Clearly, the permutation, associated with the graph  $\mathcal{L}$  on the left side of the picture, contains the identity permutation  $(x_0)$



(which leaves the first parameter  $x_0$  unchanged) combined with a permutation  $(x_4, x_6, x_5, x_2, x_3, x_1)$  of the remaining six parameters  $(x_1, x_2, x_3, x_4, x_5, x_6)$ . Using the  $Z$ -invariance, the leftmost spectral parameter line  $x_0$  can be completely disentangled from the rest of the graph, as shown on the left side of Fig. 6. Thus, the partition functions for the graphs shown on two sides of Fig. 6 coincide (more precisely, they differ from each other by some simple factors, as explained above). Recently, identities of this type were intensively studied in the context of the “lasso operator method” [38] and the “Yangian invariance” of the Zamolodchikov’s fishnet diagrams [12] in Quantum Field Theory, see [39] and references therein. Here, we just remark, that such identities could generally be obtained in a regular way as a consequence of Baxter’s  $Z$ -invariance. In Appendix B we demonstrate how this works on the example of the  $q$ -analog of the  $\mathfrak{D} = 1$  fishing-net model, obtained in this paper.

#### 4.4 Dual formulation of the model

The definition of the dual model follows the same steps as in Sec. 4.1, except that the spin variables are placed on the unshaded faces of the graph  $\mathcal{L}$ . Namely, each unshaded face is assigned with a continuous spin variable  $0 \leq \varphi_i < 2\pi$ . As before, introduce the spectral parameter ratio variable  $s_{ij}$  by the same formula (4.1). Then each vertex  $(ij) \in V(\mathcal{L})$  is assigned with the Boltzmann weight  $\rho(s_{ij}) \overline{\omega}_{s_{ij}}(\varphi_i - \varphi_j)$ , where  $\varphi_i$  and  $\varphi_j$  are the spins on the unshaded faces across the vertex, the weights  $\omega_x(\varphi)$  and  $\overline{\omega}_x(\varphi) = \omega_{\xi/x}(\varphi)$  are defined in (3.27) and  $\rho(s_{ij})$  is the normalization factor. In graphical notations one has

$$(i) : \begin{array}{c} y \\ \nearrow \\ \varphi_j \\ \searrow \\ x \\ \nearrow \\ \varphi_i \\ \searrow \end{array} = \overline{\omega}_{x/y}(\varphi_i - \varphi_j), \quad (ii) : \begin{array}{c} y \\ \nearrow \\ \varphi_i \\ \searrow \\ x \\ \nearrow \\ \varphi_j \\ \searrow \end{array} = \omega_{x/y}(\varphi_i - \varphi_j), \quad (4.11)$$

for the first (i) and second (ii) type of vertices, respectively. The partition function of the dual model is defined as an integral over all configurations of interior spins with the weight equal to the product of the local weights over all vertices of  $\mathcal{L}$ ,

$$Z^{(D)} = \int_0^{2\pi} \dots \int_0^{2\pi} \prod_{\text{interior spins}} \frac{d\varphi_i}{2\pi} \prod_{(i,j) \in V(\mathcal{L})} \rho(s_{ij}) \overline{\omega}_{s_{ij}}(\varphi_i - \varphi_j). \quad (4.12)$$

The spins on exterior faces are kept fixed.

Using the standard arguments [1] based on the duality transformation (3.25) one can relate (4.2) with (4.12). In particular, for a large lattice  $\mathcal{L}$  with  $M$  shaded faces, one obtains

$$\log Z^{(D)} = \log Z + \sum_{(i,j)} \log \frac{\sigma(s_{ij}^2)}{\kappa_s} + O(\sqrt{M}). \quad (4.13)$$

where  $\log Z$  is given by (4.3). For the homogeneous square lattice the last relation simplifies to

$$\log Z^{(D)} = \log Z - 2M \log \kappa_s + O(\sqrt{M}). \quad (4.14)$$

due to the identity  $\sigma(x^2)\sigma(-q/x^2) = 1$ .

## 5 Partition function

### 5.1 Inversion relation method

In this section we calculate the partition function of the model in the large lattice limit, using the inversion relations method [34–36]. From now on we will adopt the following normalization of the

Boltzman weights in (4.2)

$$\rho(x) = \frac{(-qx^{-2}; q^2)_\infty}{(-qx^2; q^2)_\infty}, \quad \log \rho(x) = \sum_{m=1}^{\infty} \frac{(-q)^m (x^{2m} - x^{-2m})}{m(1 - q^{2m})}. \quad (5.1)$$

It is useful to note, that

$$\rho(\xi x)\rho(\xi/x) = (1 - x^2)(1 - x^{-2}), \quad \rho(x)\rho(x^{-1}) = 1. \quad (5.2)$$

With this normalization the weights  $\rho(x)W_x(n)$  and  $\rho(\xi/x)\overline{W}_x(n)$ , with  $n \in \mathbb{Z}$ , are analytic in the ring

$$\xi^2 < |x| < \xi^{-1}, \quad 0 < \xi < 1. \quad (5.3)$$

The factor (5.1) is chosen such that

$$\rho(x)W_x(0) = \rho(\xi/x)\overline{W}_x(0) \equiv 1. \quad (5.4)$$

In view of the above, it is natural to assume, that for positive real values of  $\xi$  the edge partition function  $\kappa_e(x)$  is analytic in the ring

$$\xi e^{-\delta} < |x| < e^{\delta}, \quad 0 < \xi < 1. \quad (5.5)$$

where  $\delta > 0$  is a small, but finite constant. Then, the inversion relations (4.9), (4.10) have a unique solution,

$$\log \kappa_e(x) = \log \rho(x) - \sum_{m=1}^{\infty} \frac{(-q)^m (x^{2m} - x^{-2m})}{m(1 - q^m)(1 + (-q)^m)} = 2 \sum_{m=1,3,5,\dots}^{\infty} \frac{q^{2m}(x^{2m} - x^{-2m})}{m(1 - q^m)(1 - q^{2m})} \quad (5.6)$$

The derivation is straightforward. Taking the logarithms of (4.10) and using the Laurent series

$$\log \kappa_e(x) = \sum_{m=-\infty}^{\infty} a_m x^{2m}, \quad \log \sigma(x^2) = \sum_{m=1}^{\infty} \frac{x^{2m} - (\xi/x)^{2m}}{m(1 - q^m)} \quad (5.7)$$

one obtains a system of a linear equations for the coefficients  $\{a_m\}$ , which immediately leads to the above result (5.6). The equation (4.9) is automatically satisfied. Mention also a product representation for (5.6),

$$\kappa_e(x) = \frac{(qx^2; q^2)_\infty}{(-qx^2; q^2)_\infty} F(x) F(\xi/x), \quad F(x) = \prod_{n=1}^{\infty} \left( \frac{(1 + q^{2n}x^2)(1 - q^{2n}/x^2)}{(1 - q^{2n}x^2)(1 + q^{2n}/x^2)} \right)^n. \quad (5.8)$$

Substituting (5.6) into (4.7) one gets the partition function per site (4.4) for the case of the homogeneous square lattice model

$$\log \kappa^{(\text{sq})}(x) = \log(\kappa_s \rho(x)\rho(\xi/x)) - \sum_{m=1}^{\infty} \frac{(x^{2m} + (\xi/x)^{2m})(\xi^{2m} - 1)}{m(1 - q^m)(1 + \xi^{2m})} = \quad (5.9)$$

$$= \log \kappa_s + 2 \sum_{m=1,3,5,\dots}^{\infty} \frac{q^m (x^{2m} + (\xi/x)^{2m})}{m(1 - q^m)^2}, \quad \xi^2 = -q, \quad (5.10)$$

or in a product form

$$\kappa^{(\text{sq})}(x) = \kappa_s \frac{(qx^2, -q^2/x^2; q^2)_\infty}{(-qx^2, q^2/x^2; q^2)_\infty} F(x)^2 F(\xi/x)^2. \quad (5.11)$$

The results (5.6), (5.9) strongly resemble the expression for the partition function of the symmetric 8-vertex model [1, 5]. It is, therefore, important to better understand this connection.

## 5.2 Connection to the 8-vertex model

The  $R$ -matrix of the symmetric 8-vertex model has the form

$$\mathcal{R}^{(8v)}(u) = \begin{pmatrix} a(u) & & & d(u) \\ & b(u) & c(u) & \\ & c(u) & b(u) & \\ d(u) & & & a(u) \end{pmatrix} \quad (5.12)$$

with the Boltzmann weights parameterized as

$$\begin{aligned} a(u) &= \rho_8 \vartheta_4(\lambda) \vartheta_1(\lambda - u) \vartheta_4(u), & b(u) &= \rho_8 \vartheta_4(\lambda) \vartheta_4(\lambda - u) \vartheta_1(u), \\ c(u) &= \rho_8 \vartheta_1(\lambda) \vartheta_4(\lambda - u) \vartheta_4(u), & d(u) &= \rho_8 \vartheta_1(\lambda) \vartheta_1(\lambda - u) \vartheta_1(u). \end{aligned} \quad (5.13)$$

Here we have used the standard notations for the  $\vartheta$ -functions

$$\vartheta_1(u) = i q^{1/4} e^{-iu} (e^{2iu}, q^2 e^{-2iu}, q^2; q^2)_\infty, \quad \vartheta_4(u) = (q e^{2iu}, q e^{-2iu}, q^2; q^2)_\infty. \quad (5.14)$$

where  $\rho_8$ ,  $\lambda$ ,  $u$  and  $q$  are free parameters of the model. It is convenient to define

$$\bar{\xi} = e^{i\lambda}, \quad x = e^{iu}, \quad \gamma = i q^{1/4} (q^2; q^2)_\infty^2 \vartheta_4(0), \quad (5.15)$$

Then in the regime when  $x$  and  $\bar{\xi}$  are real and positive and

$$0 < \bar{\xi} < x < 1, \quad |q| < 1. \quad (5.16)$$

the partition function per site reads (see Eq.(10.8.44) of [1])

$$\log \kappa^{(8)}(x) = \log(\rho_8 \gamma / \bar{\xi}) - \sum_{m=1}^{\infty} \frac{(x^{2m} + (\bar{\xi}/x)^{2m})(\bar{\xi}^{-2m} + (q/\bar{\xi}^2)^m)}{m(1 - q^m)(1 + \bar{\xi}^{-2m})}. \quad (5.17)$$

Let us now identify the parameters  $x, q, \bar{\xi}$  in (5.17) with the corresponding parameters  $x, q, \xi$  in (5.9). Thereby we need to set

$$e^{2i\lambda} = \bar{\xi}^2 = \xi^2 = -q, \quad (5.18)$$

Then it is not difficult to show that the two partition functions differ from each other by a simple factor

$$\kappa^{(8)}(x) / \kappa^{(sq)}(x) = \frac{\rho_8 \gamma (-x^2, qx^{-2}; q)_\infty}{\xi \kappa_s}. \quad (5.19)$$

where the normalization factor (5.1) is taken into account. Thus, the new infinite-state model (1.9), introduced in this paper, is “weakly-equivalent” to the 8-vertex model. Interestingly, the arising correspondence leads to an unphysical regime of the 8-vertex model, where the weight  $d(u)$  in (5.13) is purely imaginary, if  $a(u), b(u)$  and  $c(u)$  are chosen to be real and positive. However, the infinite state-model on the other side of the correspondence has strictly positive Boltzmann weights.

Next, we observe, that with the relation (5.18) between  $\lambda$  and  $q$  the 8-vertex model (5.13) reduces to the free fermion model [40, 41] with the condition<sup>6</sup>

$$a^2 + b^2 - c^2 - d^2 = 0, \quad (5.20)$$

for the Boltzmann weights. Moreover, it is worth noting that the site factor

$$\kappa_s = \frac{(q; q)_\infty}{(-q; q)_\infty} = (q; q^2)_\infty^2 (q^2; q^2)_\infty = \vartheta_4(0) = \vartheta_4 \quad (5.21)$$

<sup>6</sup>In general the weights (5.13) satisfy the condition

$$\frac{a^2 + b^2 - c^2 - d^2}{ab} = -\frac{2 \vartheta_4^2 \vartheta_2(\lambda) \vartheta_3(\lambda)}{\vartheta_2 \vartheta_3 \vartheta_4^2(\lambda)}.$$

In the case (5.18) the function  $\vartheta_3(\lambda)$  vanishes.

is just a theta constant. The partition function (5.17) can now be written as a 2D free-fermion determinant [40]

$$\log \kappa^{(8)} = \frac{1}{8\pi^2} \int_0^{2\pi} \int_0^{2\pi} d\phi_1 d\phi_2 \log \left| 2A + 2D \cos(\phi_1 - \phi_2) + 2E \cos(\phi_1 + \phi_2) \right| \quad (5.22)$$

where

$$A = a^2 + b^2, \quad D = c^2 - a^2, \quad E = d^2 - a^2, \quad (5.23)$$

which is simply related to the partition function of the 2D zero-field Ising model [2]. The product representations of the type (5.11) for the most general free-fermion model and the equivalent checkerboard Ising model were obtained in [42, 43].

### 5.3 Critical point

Let us now analyse the behavior of the model near the critical point  $\mathbf{q} = -1$ , where the model exhibits a phase transition. Let

$$\xi = e^{-\epsilon/2}, \quad \mathbf{q} = -e^{-\epsilon}, \quad x^2 = e^{-\theta\epsilon}, \quad \epsilon \rightarrow +0. \quad (5.24)$$

where  $\theta$  is a new parameter, replacing  $x$ . Then for the normalized Boltzmann weights (5.4) of the discrete spin model for  $\epsilon \rightarrow 0$ , one obtains,

$$\frac{W_x(2n)}{W_x(0)} = V_\theta(n) + O(\epsilon), \quad \frac{\overline{W}_x(2n)}{\overline{W}_x(0)} = V_{1-\theta}(n) + O(\epsilon) \quad (5.25)$$

where  $n \in \mathbb{Z}$

$$V_\theta(n) = \frac{\Gamma(\frac{1+\theta}{2}) \Gamma(n + \frac{1-\theta}{2})}{\Gamma(\frac{1-\theta}{2}) \Gamma(n + \frac{1+\theta}{2})}. \quad (5.26)$$

such that for large  $n$

$$\log V_\theta(n) = -\theta \log |n| + O(1) + O(n^{-1} \log |n|), \quad n \gg 1. \quad (5.27)$$

For odd values of spins

$$\frac{W_x(2n+1)}{W_x(0)} = \epsilon^\theta (1 + O(\epsilon)), \quad \frac{\overline{W}_x(2n+1)}{\overline{W}_x(0)} = \epsilon^{1-\theta} (1 + O(\epsilon)). \quad (5.28)$$

For the dual (compact) formulation of the model one obtains,

$$\omega_x(\varphi) = \mathbf{w}_\theta(\varphi) + O(\epsilon), \quad \overline{\omega}_x(\varphi) = \mathbf{w}_{1-\theta}(\varphi) + O(\epsilon), \quad (5.29)$$

where

$$\mathbf{w}_\theta(\varphi - \varphi') = |2 \sin(\varphi - \varphi')|^{-\theta} \quad (5.30)$$

Note that the weights (5.25) and (5.30) describe the  $N \rightarrow \infty$  limit [44] of the Fateev-Zamolodchikov  $Z_N$  model [10], which is equivalent to  $\mathfrak{D} = 1$  Zamolodchikov's fishing-net model <sup>7</sup>.

With the parameterization (5.24) the function  $F(x)$  defined in (5.8) has the following asymptotics when  $\epsilon \rightarrow 0$ ,

$$F(x) = e^{-\frac{\pi^2}{8\epsilon}\theta} G(\theta) \left( 1 - \frac{\pi}{\epsilon} e^{-\pi^2/\epsilon} \sin \pi\theta + O(\epsilon) \right) \quad (5.31)$$

where

$$G(\theta) = \exp \left\{ \frac{1}{\pi} \int_0^{\pi\theta/2} (x \cot x) dx \right\} = e^{\frac{1}{2}\theta} \prod_{n=1}^{\infty} \left( \frac{\Gamma(n + \frac{\theta}{2})}{\Gamma(n - \frac{\theta}{2})} e^{-\theta\psi(n)} \right), \quad G(1) = \sqrt{2}, \quad (5.32)$$

<sup>7</sup>The formulation of [12] (with continuous spin variables on the real line  $x, x' \in \mathbb{R}$ ) with the Boltzmann weights proportional to  $\sim |x - x'|^{-\theta}$  is connected to (5.30) by the transformation  $x = \cot \varphi$ ,  $x' = \cot \varphi'$ .

and  $\psi(x) = d \log \Gamma(x)/dx$  is the logarithmic derivative of the gamma-function. In writing (5.31) we have indicated the most singular non-analytic correction term, though numerically it could be much smaller than the regular  $O(\epsilon)$  term. It follows then that partition function (5.9) has the following expansion when  $\epsilon \rightarrow 0$ ,

$$\log \kappa^{(\text{sq})}(x) = \log \kappa_0^{(\text{sq})}(\theta) + \log \kappa_{\text{reg}}^{(\text{sq})}(\theta) + \log \kappa_{\text{sing}}^{(\text{sq})}(\theta) + \dots \quad (5.33)$$

The leading term is given by

$$\kappa_0^{(\text{sq})}(\theta) = \frac{\Gamma(1 - \frac{\theta}{2})\Gamma(\frac{1+\theta}{2})}{\pi} \mathbf{Z}(\theta)^2, \quad (5.34)$$

where

$$\begin{aligned} \mathbf{Z}(\theta) &= \mathbf{Z}(1 - \theta) = \prod_{n=1}^{\infty} \frac{\Gamma(n + \frac{\theta}{2})\Gamma(n + \frac{1-\theta}{2})\Gamma(n - \frac{1}{2})}{\Gamma(n - \frac{\theta}{2})\Gamma(n - \frac{1-\theta}{2})\Gamma(n + \frac{1}{2})} \\ &= \sqrt{\cos \frac{\pi\theta}{2}} \exp \left( \frac{1}{8} \int_{\mathbb{R}} \frac{dw}{w} \frac{\sinh(2\theta w)}{\cosh^2(w)} \right) \\ &= \exp \left\{ \frac{1}{16\pi^2} \int_0^{2\pi} \int_0^{2\pi} d\phi_1 d\phi_2 \log \left( 2 + 2 \sin^2(\pi\theta/2) \cos(\phi_1 - \phi_2) - 2 \cos^2(\pi\theta/2) \cos(\phi_1 + \phi_2) \right) \right\} \end{aligned} \quad (5.35)$$

is the partition function per edge for  $\mathfrak{D} = 1$  Zamolodchikov's fishing net model presented in three different forms. Next, the term  $\log \kappa_{\text{reg}}^{(\text{sq})}(\theta)$  stands for a well defined regular series in positive integer powers of  $\epsilon$  vanishing in the limit  $\epsilon \rightarrow 0$ , and  $\log \kappa_{\text{sing}}^{(\text{sq})}$  denotes the most singular non-analytic contribution near  $\epsilon \sim 0$

$$\log \kappa_{\text{sing}}^{(\text{sq})} = -\frac{4\pi}{\epsilon} e^{-\pi^2/\epsilon} \sin \pi\theta. \quad (5.36)$$

The dots in (5.33) denote less singular terms of the order  $O(\tilde{\mathfrak{q}}^n)$  and  $O(\tilde{\mathfrak{q}}^{n+1} \log \tilde{\mathfrak{q}})$  with  $n \geq 1$ , where  $\tilde{\mathfrak{q}} = e^{-\pi^2/\epsilon}$ .

The first line in (5.35) is the original result of [12]. The second line is (the square root of) the partition function per site of the six-vertex model at the free-fermion point and the third line is its free-fermion determinant representation, see Appendix C for additional details. As a side remark note, that the partition function of the general fishing-net model [12], where the spins are taking values in  $\mathbb{R}^2$  with  $\mathfrak{D} \geq 1$ , can be represented as a product of the same determinants (5.35) with shifted values of the spectral parameter  $\theta$ .

## 6 Conclusion

In this paper we obtained a new solution of the star-triangle relation with positive Boltzmann weights. The solution is presented to two equivalent forms: the non-compact form, with spins taking arbitrary integer values and the compact form, with continuous spins taking values on the circle  $0 \leq \varphi < 2\pi$ . It is commonly accepted that the solutions of the Yang-Baxter equation (with the star-triangle relation being a particular case) are completely described by the theory of quantum groups [45–47], so finding a new solution should, in principle, be reducible to a routine task of the representation theory. From the algebraic point of view the new solution is closely related to the six-vertex model. It is, indeed, connected with the problem of the construction of an intertwiner for two particular infinite-dimensional representations of the quantum affine algebra  $U_q(\widehat{sl}(2))$ , which is the simplest and most well studied quantum affine algebra. However, the fact that this solution has not so far been discovered indicates that the problems of the representation theory, perhaps, are not so routine. Indeed, a more rigorous consideration of the recurrence relations for the Boltzmann weights (1.7) has led to non-hypergeometric type summation formulae, e.g., the star-triangle equation (1.4) itself

and the generalized Ramanujan  ${}_1\psi_1$  summation formula (3.28). It would be interesting to explore application of these ideas to other algebras.

We also presented an exactly solvable two-dimensional lattice model describing interaction of integer-valued spins  $a, b, \dots$  (often called “heights”) on the neighbouring sites of the square lattice. It can be viewed as a discrete solid-on-solid (SOS) model for a surface roughening transition. The model

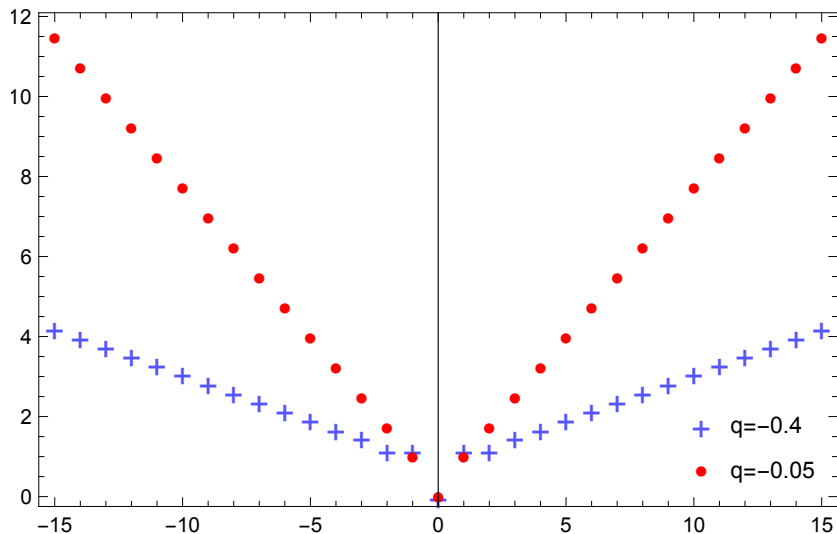


**Figure 7:** The two-spin interaction energy  $\beta E(a, b) = -\log(W_{\sqrt{\xi}}(a-b)/W_{\sqrt{\xi}}(0))$  for the discrete SOS model, as a function of the spin difference  $(a-b)$ . The linear growth at large arguments is described by (6.1).

have one temperature-like parameter  $q = -\xi^2$ ,  $0 < \xi < 1$ . In the symmetric case (with the same interaction on the horizontal and vertical edges) the two-spin interaction energy multiplied by the inverse temperature, illustrated in Fig. 7, can be approximated by a simplified formula

$$\beta E(a, b) = -\log \frac{W_{\sqrt{\xi}}(a-b)}{W_{\sqrt{\xi}}(0)} \sim -\frac{1}{2}|a-b| \log \xi, \quad |a-b| \gg 1. \quad (6.1)$$

So the parameter  $-\log \xi$  plays the role of the inverse temperature. At small  $\xi$  one expects an ordered state, while at  $\xi \sim 1$  the linear interaction disappears, so the spins are expected to be disordered (to avoid confusions, note that at  $\xi = 1$  the formula (6.1) is not applicable, see Eqs. (5.25), (5.27) and (5.28) in the main text). From the exact result (5.9) for the partition function of the model it follows, that the most singular contribution to the free energy near the critical point  $\xi = 1$ , is given by (5.36),

$$\log \kappa_{\text{sing}}^{(\text{sq})} \sim -\frac{4\pi}{\epsilon} e^{-\pi^2/\epsilon}, \quad \xi = e^{-\epsilon/2}, \quad \epsilon \rightarrow 0, \quad (6.2)$$

which, with an account of (5.25), indicates an infinite order phase transition. At the critical point the model reduces to the  $\mathfrak{D} = 1$  Zamolodchikov’s fishing-net model [12].

In the dual formulation the spins take continuous values on the circle  $0 \leq \varphi_i < 2\pi$  and the neighbouring spin interaction energy  $\beta E^{(D)}(\varphi)$  becomes a  $2\pi$ -periodic and even function of the spin difference  $\varphi = \varphi_i - \varphi_j$ . It is illustrated in Fig. 8. For small  $q = -\xi^2$  the interaction energy is just a weakly oscillating function

$$\beta E^{(D)}(\varphi) = -\log \omega_{\sqrt{\xi}}(\varphi) = -2\sqrt{\xi} \cos \varphi + O(\xi), \quad \xi \sim 0, \quad (6.3)$$

but when  $\xi \rightarrow 1$  it develops two sharp and gradually deepening minima at  $\varphi = 0$  and  $\varphi = \pi$  (see Fig. 8 and Eq.(5.30) for the limiting form of the weight  $\omega_x(\varphi)$  at  $\xi = 1$ ). It would be interesting to verify (for instance, using the approach of [48]) whether the phase transition in the model could be interpreted

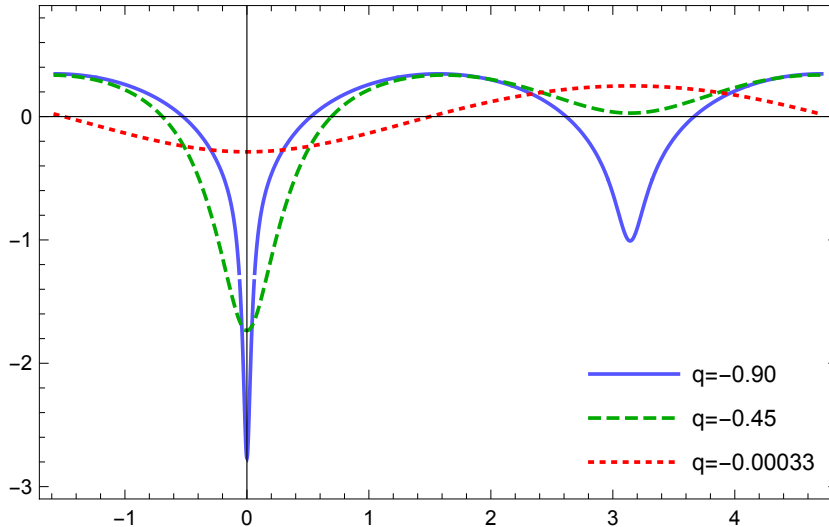


**Figure 8:** The two-spin interaction energy  $\beta E^{(D)}(\varphi) = -\log \omega_{\sqrt{\xi}}(\varphi)$  as a function of the spin difference  $\varphi$  in the dual formulation of the model.

as a Berezinskii-Kosterlitz-Thouless transition [49, 50] induced by contributions of vortex/antivortex configurations to the partition function. Moreover, it would be useful to calculate the spin correlation functions, which we postpone to a future publication.

Finally, mention an intriguing connection of the partition function of the model with the partition function of the off-critical 8-vertex free-fermion model. Essentially, the two partition function coincide (more precisely, they differ by a simple factor which can be absorbed into the normalization of the Boltzmann weights). This means that the partition function of the model can be represented as a free-fermion determinant. It would be extremely interesting to understand this connection on the level of the Bethe ansatz.

## Acknowledgements

The authors thank R. J. Baxter, R. M. Kashaev, S. L. Lukyanov, J. H. H. Perk, V. P. Spiridonov and S. O. Warnaar for very stimulating discussions at various stages of this work. SMS acknowledges the support of the Australian Research Council grant DP190103144.

## Appendix A. Solution of the recurrence and inversion relations

Consider a subset of (3.19), (3.20) and (3.22) only involving the weight  $\overline{W}_x(n)$ ,

$$\frac{\overline{W}_x(n)}{\overline{W}_x(n-2)} = \left(-\frac{\mathbf{q}}{x^2}\right) \frac{(1 - \mathbf{q}^{n-2} x^2)}{(1 - \mathbf{q}^n/x^2)}, \quad (\text{A.1})$$

$$\sum_{n \in \mathbb{Z}} \overline{W}_x(a-n) \overline{W}_{1/x}(n-b) \simeq \delta_{a,b}, \quad \overline{W}_x(n) \overline{W}_{-\mathbf{q}/x}(n) \simeq 1, \quad a, b, n \in \mathbb{Z}, \quad (\text{A.2})$$

Introduce the notation

$$w_x(n) = \begin{cases} w_x(0), & n = \text{even}, \\ w_x(1), & n = \text{odd}. \end{cases} \quad (\text{A.3})$$

where  $w_x(0)$  and  $w_x(1)$  are two arbitrary functions of  $x$ . Then, the most general solution of (A.1) for  $\overline{W}_x(n)$  can be written as

$$\overline{W}_x(n) = w_x(n) \left(\frac{\xi}{x}\right)^n \frac{(\mathbf{q}^{2+n}/x^2; \mathbf{q}^2)_\infty}{(\mathbf{q}^n x^2; \mathbf{q}^2)_\infty} \quad (\text{A.4})$$

where  $(x; \mathfrak{q}^2)_\infty$  denotes the  $\mathfrak{q}$ -Pochhammer symbol

$$(x; \mathfrak{q}^2)_\infty = \prod_{k=0}^{\infty} (1 - x \mathfrak{q}^{2k}). \quad (\text{A.5})$$

Substituting this into the first equation in (A.2) one obtains an infinite set of equations of the form

$$\begin{aligned} A_x(a-b) w_x(0) w_{1/x}(0) + B_x(a-b) w_x(1) w_{1/x}(1) &= 0, & a-b &= \pm 2, \pm 4, \dots, \\ C_x(a-b) w_x(0) w_{1/x}(1) + D_x(a-b) w_x(1) w_{1/x}(0) &= 0, & a-b &= \pm 1, \pm 3, \dots \end{aligned} \quad (\text{A.6})$$

where the coefficients  $A, B, C, D$  are known function of the spectral variable  $x$  and the spin difference (they can be explicitly calculated using the Ramanujan bilateral summation formula  ${}_1\psi_1$ ). A careful analysis shows that all these equations are consistent and reduce to only two equations

$$\begin{aligned} w_x(0) w_{1/x}(0) - w_x(1) w_{1/x}(1) &= 0, \\ w_x(0) w_{1/x}(1) - w_x(1) w_{1/x}(0) &= 0, \end{aligned} \quad (\text{A.7})$$

which have a simple solution  $w_x(1) = \pm w_x(0)$ . Therefore, we will set

$$w_x(1) = w_x(0) = 1, \quad \forall n, \quad (\text{A.8})$$

which fixes  $\overline{W}_x(n)$  to within an overall normalization and a trivial equivalence transformation  $\overline{W}_x(n) \rightarrow (-1)^n \overline{W}_x(n)$ . Then, using (A.1) together with (A.8) one can easily check that the second relation in (A.2) is automatically satisfied

$$\overline{W}_x(n) \overline{W}_{-\mathfrak{q}/x}(n) = 1. \quad (\text{A.9})$$

Similar considerations apply to the weight function  $W_x(n)$ . The results are presented in (3.14) of the main text.

## Appendix B. Factorization of the partition function

In Sect.4.3 we have considered an example of the planar graph  $\mathcal{L}$ , where one spectral parameter line (the leftmost line in Fig. 6) could be completely disentangled from the rest of the graph by using the  $Z$ -invariance. Here we present a more detailed description of yet another example of this sort.

The definition of the  $Z$ -invariant models formulated in Sect. 4.1 above can be generalized by including additional types of lines. For instance, the six-vertex type lines carrying two-state spins, which have already appeared in Sect. 3.1. Graphically, they are represented as thick directed lines, which are continued as dashed lines in the shaded areas. Their intersections with the thin spectral parameter lines together with the associated tri-spin weights are shown in (3.7) and (3.8) (the weights are defined in (3.2), (3.4)).

Apart from adding the new type of lines, we will also slightly relax the requirements on the topology of the graph  $\mathcal{L}$  discussed in Sect. 4.1. This graph is formed by a set of directed spectral parameter lines, which go from the bottom of the graph to the top, intersecting one another on the way. To formalize this one can say that the lines start at the bottom side of a rectangular strip and end up at its top side. Let us now relax this by allowing the lines (i) to start from the bottom or the lateral sides of the strip, (ii) to end up at at the top or the lateral sides of the strip. However, as before, there should be no closed directed paths. As an example, consider the graph presented on the left side of Fig. 9 (we assume that the line  $x_1$  is ending at the right side of the strip, while the line  $x_2$  is starting from it). It is easy to check that there are no closed directed loops, so that the graph satisfy all the above conditions.

Next, we use the graphic rules (3.7), (3.8) and (3.10) to assign Boltzmann weights to all vertices in Fig. 9. The partition function is defined as a sum over all configurations of interior spins (in this case



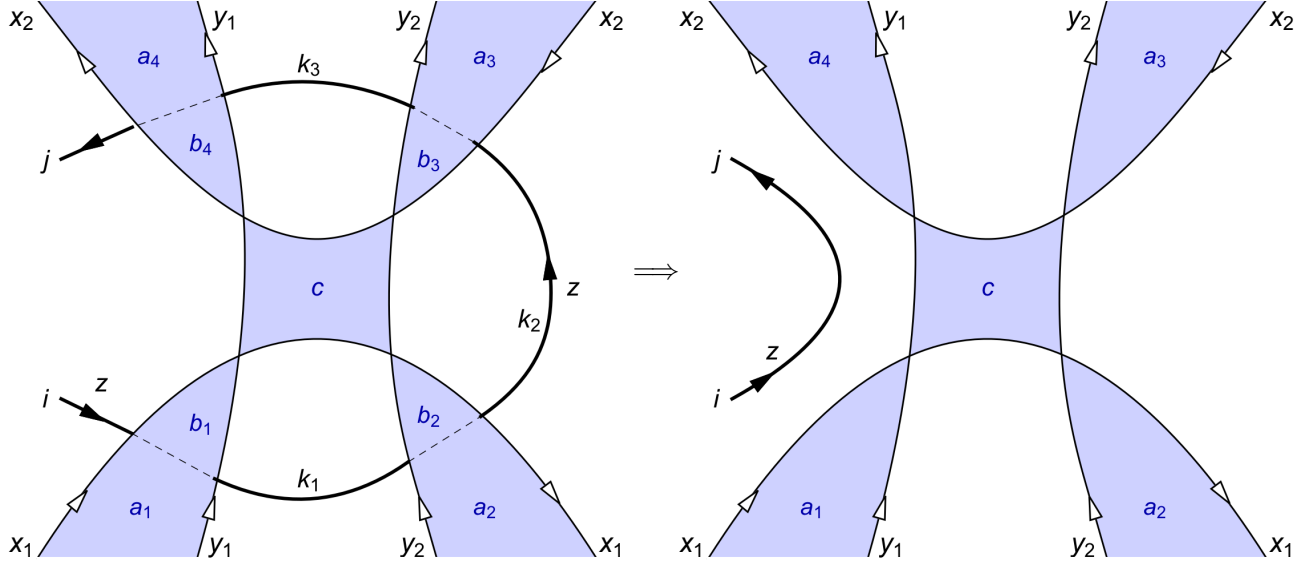


**Figure 9:** An example of planar graphs connected with each other by the Yang-Baxter type and inversion relation moves. Their partition functions differ by simple factors, see (B.16)

$b_1, b_2, b_3, b_4, c \in \mathbb{Z}$  and  $k_1, k_2, k_3 = \pm 1$ ) with the weight equal to the product of the local weights over all vertices. Note, that the vertex weights only depend on the relative orientation of the directed lines among themselves and with respect to the shaded faces. They are not affected by overall rotations of the vertices. Therefore, the partition function of the graph will not change, if the graph is deformed without changing its topology. In this way the graph on the left side of Fig. 9 can be transformed

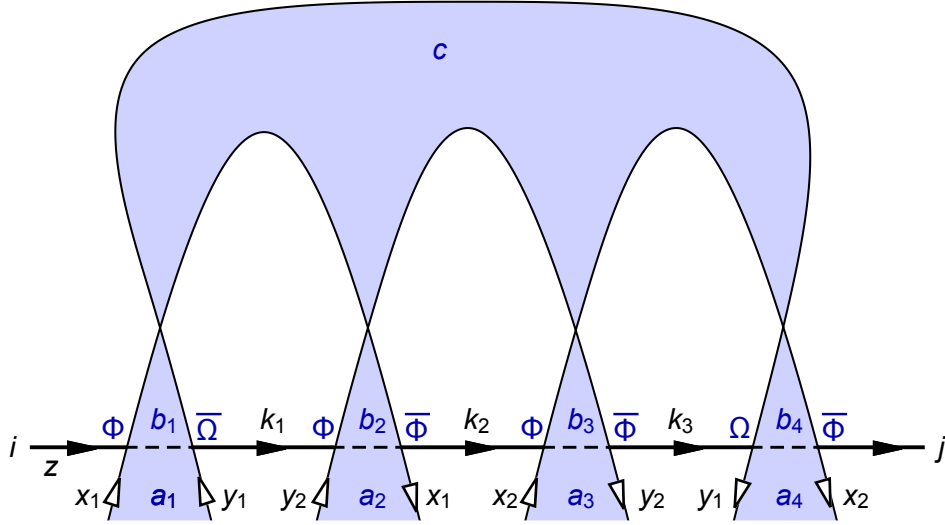


**Figure 10:** An equivalent transformation of the graph shown on the left side of Fig. 9. Note, that all lines in the new graph are heading in the same direction: from left to right.

into an equivalent graph shown in Fig. 10. Its partition function reads

$$\mathcal{Z} = \sum_{b_1, b_2, b_3, b_4 \in \mathbb{Z}} (\mathcal{M}(x_1, x_2, y_1, y_2 | z)_{a_1, a_2, a_3, a_4}^{b_1, b_2, b_3, b_4})_{i, j} \mathcal{V}(x_1, x_2, y_1, y_2)_{b_1, b_2, b_3, b_4} \quad (\text{B.1})$$

where

$$\mathcal{V}(x_1, x_2, y_1, y_2)_{b_1, b_2, b_3, b_4} = \sum_{c \in \mathbb{Z}} \bar{W}_{x_1/y_1}(b_1 - c) W_{x_1/y_2}(b_2 - c) W_{y_2/x_2}(b_3 - c) \bar{W}_{y_1/x_2}(b_4 - c), \quad (\text{B.2})$$

combines contributions of the two-spin weights, as defined in (3.10) (top part of Fig. 10) and

$$\begin{aligned}
(\mathcal{M}(x_1, x_2, y_1, y_2 | z)_{a_1, a_2, a_3, a_4}^{b_1, b_2, b_3, b_4})_{i, j} &= \sum_{k_1, k_2, k_3 = \pm 1} \Phi(x_1, z)_{a_1, i}^{b_1} \bar{\Omega}(y_1, z)_{a_1, k_1}^{b_1} \Phi(y_2, z)_{a_2, k_1}^{b_2} \bar{\Phi}(x_1, z)_{a_2, k_2}^{b_2} \times \\
&\quad \times \Phi(x_2, z)_{a_3, k_2}^{b_3} \bar{\Phi}(y_2, z)_{a_3, k_3}^{b_3} \Omega(y_1, z)_{a_4, k_3}^{b_4} \bar{\Phi}(x_2, z)_{a_4, j}^{b_4}, \tag{B.3}
\end{aligned}$$

combines the tri-spin weights, graphically defined in (3.7), (3.8) (bottom part of Fig. 10). Note, that the last expression could be viewed as matrix elements of a (column-inhomogeneous) monodromy matrix

$$\begin{aligned}
(\mathcal{M}(x_1, x_2, y_1, y_2 | z)_{a_1, a_2, a_3, a_4}^{b_1, b_2, b_3, b_4})_{i, j} &= \\
&= \sum_{k_1, k_2, k_3} (\mathcal{L}(x_1, y_1, z)_{a_1}^{b_1})_{i, k_1} (\mathcal{L}(y_2, x_1/\xi, z)_{a_2}^{b_2})_{k_1, k_2} (\mathcal{L}(x_2, y_2/\xi, z)_{a_3}^{b_3})_{k_2, k_3} (\mathcal{L}(y_1/\xi, x_2/\xi, z)_{a_4}^{b_4})_{k_3, j}. \tag{B.4}
\end{aligned}$$

with  $i, j = \pm 1$ . In writing the last formula we have used (3.4) and (3.6). It is a two-by-two matrix  $\mathcal{M}(x_1, x_2, y_1, y_2 | z)$  with operator-valued elements acting the ‘‘quantum space’’  $\mathbb{Z}^4$ . From (2.2) it follows that

$$\sum_{j_1, j_2 = \pm 1} \mathcal{M}(z_1)_{i_1, j_1} \mathcal{M}(z_2)_{i_2, j_2} \mathcal{R}^{(6v)}(z_1^2/z_2^2)_{j_1, j_2}^{k_1, k_2} = \sum_{j_1, j_2 = \pm 1} \mathcal{R}^{(6v)}(z_1^2/z_2^2)_{i_1, i_2}^{j_1, j_2} \mathcal{M}(z_2)_{j_2, k_2} \mathcal{M}(z_1)_{j_1, k_1}, \tag{B.5}$$

where we have omitted the arguments  $\{x_1, x_2, y_1, y_2\}$ , which are the same for  $\mathcal{M}(z_1)$  and  $\mathcal{M}(z_2)$ .

Consider now further equivalence transformations of the graph in Fig.10 by moving the thick horizontal  $z$ -line upwards through the intersections of the thin lines to the position shown in Fig. 11. In doing this we need to use three similar, but slightly different, Yang-Baxter type moves. The first

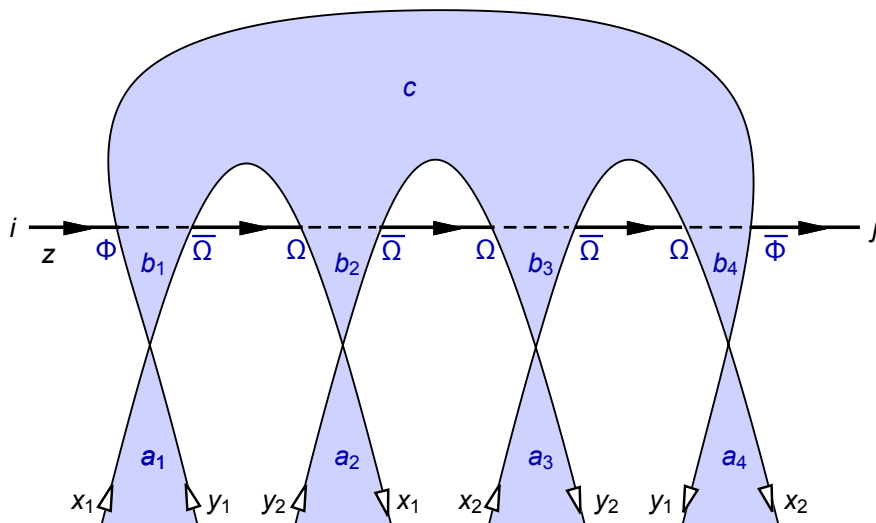


**Figure 11:** The graph obtained from Fig. 10 by four Yang-Baxter type moves, shown in (B.7), (B.10) and (B.12).

one is based on the relation (3.12), which for readers’ convenience we reproduce here

$$\sum_b \Phi(x, z)_{a, i}^b \bar{\Omega}(y, z)_{a, i'}^b \bar{W}_{x/y}(b - c) = \sum_b \bar{W}_{x/y}(a - b) \Phi(y, z)_{b, i}^c \bar{\Omega}(x, z)_{b, i'}^c. \tag{B.6}$$

It can be represented graphically as

Diagram (B.7) shows two equivalent configurations of a graph. The left configuration has a central region 'b' bounded by lines 'c' (top), 'a' (bottom), and a dashed line 'z' (left and right). A horizontal line 'i' is labeled with 'Φ' and 'z', and a horizontal line 'i'' is labeled with 'Ω' and 'z'. The right configuration is identical but the horizontal lines are swapped: 'i' is labeled with 'z' and 'Φ', and 'i'' is labeled with 'z' and 'Ω'. The regions 'a' and 'c' are shaded blue.

It is worth noting that (B.6) can be rewritten as

$$\sum_b (\mathcal{L}(x, y, z))_a^b \bar{W}_{x/y}(b - c) = \sum_b \bar{W}_{x/y}(a - b) (\mathcal{L}(y, x, z))_b^c. \quad (\text{B.8})$$

The other two required relations are simple corollaries of (B.6), namely,

$$\sum_b \Phi(x, z)_{a,i}^b \bar{\Phi}(y, z)_{a,i'}^b W_{y/x}(b - c) = \sum_b W_{y/x}(a - b) \Omega(y, z)_{b,i}^c \bar{\Omega}(x, z)_{b,i'}^c, \quad (\text{B.9})$$

which is represented as

Diagram (B.10) shows two equivalent configurations of a graph. The left configuration has a central region 'b' bounded by lines 'c' (top), 'a' (bottom), and a dashed line 'z' (left and right). A horizontal line 'i' is labeled with 'Φ' and 'z', and a horizontal line 'i'' is labeled with 'Φ' and 'z'. The right configuration is identical but the horizontal lines are swapped: 'i' is labeled with 'z' and 'Ω', and 'i'' is labeled with 'z' and 'Ω'. The regions 'a' and 'c' are shaded blue.

and

$$\sum_b \Omega(x, z)_{a,i}^b \bar{\Phi}(y, z)_{a,i'}^b \bar{W}_{x/y}(b - c) = \sum_b \bar{W}_{x/y}(a - b) \Omega(y, z)_{b,i}^c \bar{\Phi}(x, z)_{b,i'}^c, \quad (\text{B.11})$$

represented as

Diagram (B.12) shows two equivalent configurations of a graph. The left configuration has a central region 'b' bounded by lines 'c' (top), 'a' (bottom), and a dashed line 'z' (left and right). A horizontal line 'i' is labeled with 'Ω' and 'z', and a horizontal line 'i'' is labeled with 'Φ' and 'z'. The right configuration is identical but the horizontal lines are swapped: 'i' is labeled with 'z' and 'Ω', and 'i'' is labeled with 'z' and 'Φ'. The regions 'a' and 'c' are shaded blue.

Taking into account (3.4) and (3.18) it is easy to see that (B.9) follows from (B.6) with the substitution  $y \rightarrow y/\xi$ . Similarly, (B.11) is obtained from (B.6) with  $x \rightarrow x/\xi$  and  $y \rightarrow y/\xi$ .

Next, we continue moving the  $z$ -line in Fig. 11 further upwards to completely detach it from the rest of the graph. To do this we will use the inversion relations (see (3.3) and (3.5) of the main text)

$$\sum_{i=\pm 1} \bar{\Omega}(x, z)_{a,i}^{a'} \Omega(x, z)_{b,i}^{a'} = [x^2/z^2] \delta_{a,b}, \quad \sum_{a' \in \mathbb{Z}} \Phi(x, z)_{a,i}^{a'} \bar{\Phi}(x, z)_{a,i'}^{a'} = [x^2/z^2] \delta_{i,i'}. \quad (\text{B.13})$$

with the notation  $[x] = x - 1/x$ . The first of them is represented as

$$\text{[Diagram with regions } a, a', b \text{ and parameters } z, i, \bar{\Omega}, \Omega, x \text{]} = [x^2/z^2] \text{[Diagram with regions } a, a', b \text{ and parameters } z, x \text{]} \quad (\text{B.14})$$

and the second one as

$$\text{[Diagram with regions } a, a' \text{ and parameters } z, i, \Phi, \bar{\Phi}, x \text{]} = [x^2/z^2] \text{[Diagram with regions } a \text{ and parameters } z, i, x \text{]} \quad (\text{B.15})$$

Proceeding in this way one obtains for the partition function (B.1),

$$\begin{aligned}
 \mathcal{Z} &= \sum_{\{b\}} \left( \mathcal{M}(x_1, x_2, y_1, y_2 | z_2)_{\{a\}}^{\{b\}} \right)_{i,j} \mathcal{V}(x_1, x_2, y_1, y_2)_{\{b\}} \\
 &= \delta_{i,j} [x_1^2/z^2] [x_2^2/z^2] [y_1^2/z^2] [y_2^2/z^2] \mathcal{V}(x_1, x_2, y_1, y_2)_{\{a\}}
 \end{aligned} \quad (\text{B.16})$$

where  $\{a\} = \{a_1, a_2, a_3, a_4\}$  and similarly for  $\{b\}$ . It is not difficult to see that up to the scalar factor the RHS of the last relation precisely reduces to the partition function of the graph shown on the right side of Fig. 9. Obviously, the quantity (B.2) can be regarded as an eigenvector of the monodromy matrix (B.3). Similar results for the Yangian case were obtained in [38].

## Appendix C. The 8-vertex free-fermion model

Note, that when

$$\mathbf{q} = -e^{-\epsilon}, \quad \epsilon \rightarrow 0, \quad \epsilon > 0, \quad (\text{C.1})$$

the 8-vertex model becomes critical [1]. Moreover, in our case (5.18) we also have the relation

$$\bar{\xi} = e^{i\lambda}, \quad \lambda = \frac{1}{2}i\epsilon. \quad (\text{C.2})$$

To study this point it is convenient to express the weights (5.13) in terms of the theta functions

$$\Theta_i(v) = \vartheta_i(v, \tilde{\mathbf{q}}), \quad (\text{C.3})$$

of the nome  $\tilde{\mathbf{q}}$  and the variable  $v$ ,

$$\tilde{\mathbf{q}} = e^{-\pi^2/\epsilon}, \quad v = -i\pi u/\epsilon. \quad (\text{C.4})$$

Using the standard formulae for transformations of the elliptic functions for the weights (5.13), one obtains,

$$\begin{aligned}
 \mathbf{a} &= \rho'_8(v) \Theta_4 \Theta_2(v) \Theta_3(v), & \mathbf{b} &= \rho'_8(v) \Theta_4 \Theta_1(v) \Theta_4(v), \\
 \mathbf{c} &= \rho'_8(v) \Theta_2 \Theta_3(v) \Theta_4(v), & \mathbf{d} &= i\rho'_8(v) \Theta_2 \Theta_1(v) \Theta_2(v).
 \end{aligned} \quad (\text{C.5})$$

where

$$\rho'_8(v) = \rho_8 \left( \frac{\epsilon}{\pi} \right)^{-3/2} \exp \left\{ + \frac{3i\pi}{4} + \frac{\epsilon}{2} - \frac{2\epsilon v(\pi/2 - v)}{\pi^2} \right\} \quad (\text{C.6})$$

In the leading order at  $\epsilon \rightarrow 0$ , one obtains

$$\begin{aligned} \mathbf{a} &= \rho_8'' \cos v, & \mathbf{b} &= \rho_8'' \sin v, \\ \mathbf{c} &= \rho_8'', & \mathbf{d} &= 0, \end{aligned} \tag{C.7}$$

which is the six-vertex free-fermion model (the ratio  $\mathbf{d}/\mathbf{c}$  in this limit vanishes as  $\exp(-\pi^2/2\epsilon)$ ). Here

$$\rho_8'' = 2\rho_8 \left(\frac{\epsilon}{\pi}\right)^{-3/2} \exp\left\{-\frac{\pi^2}{4\epsilon} + \frac{3i\pi}{4}\right\}, \tag{C.8}$$

With (C.7) the partition function (5.22) becomes

$$\begin{aligned} \log \kappa^{(8)} &= \log \rho_8'' + \frac{1}{8\pi^2} \int_0^{2\pi} \int_0^{2\pi} d\phi_1 d\phi_2 \log\left(2 + 2\sin^2 v \cos(\phi_1 - \phi_2) - 2\cos^2 v \cos(\phi_1 + \phi_2)\right) + O(\epsilon) \\ &= \log \rho_8'' + \frac{1}{4\pi} \int_0^{2\pi} d\phi \log\left(1 + \sin(2v) |\cos \phi|\right) + O(\epsilon), \end{aligned} \tag{C.9}$$

Evaluating the integral and replacing the variable  $v$  by a new variable  $\theta = 2v/\pi$ , one obtains

$$\kappa^{(8)} = \frac{\rho_8'' G^2(\theta) G^2(1-\theta)}{G^2(1)} (1 + O(\epsilon)), \quad \theta = \frac{2v}{\pi}, \tag{C.10}$$

where

$$G(\theta) = \exp\left\{\frac{1}{\pi} \int_0^{\pi\theta/2} (x \cot x) dx\right\} = e^{\frac{1}{2}\theta} \prod_{n=1}^{\infty} \left(\frac{\Gamma(n + \frac{\theta}{2})}{\Gamma(n - \frac{\theta}{2})} e^{-\theta\psi(n)}\right) \tag{C.11}$$

and  $\psi(x) = d \log \Gamma(x)/dx$  is the logarithmic derivative of the gamma-function. On the other hand, the same result should, of course, follow from the general expression of the partition function of the 8-vertex model (5.17) or from the corresponding expression for the six-vertex model (C.7) (with  $v = \pi\theta/2$ ). Indeed, using Eq.(8.8.17) from [1], one obtains

$$\kappa^{(8)} = \rho_8'' \cos(\pi\theta/2) \exp\left(\frac{1}{4} \int_{\mathbb{R}} \frac{dw}{w} \frac{\sinh(2\theta w)}{\cosh^2(w)}\right) (1 + O(\epsilon)), \quad \epsilon \rightarrow 0. \tag{C.12}$$

## References

- [1] R. J. Baxter, “Exactly solved models in statistical mechanics,” Academic: London, 1982.
- [2] L. Onsager, “Crystal statistics. I. A two-dimensional model with an order-disorder transition,” *Phys. Rev.* **65** (1944) 117–149.
- [3] J. B. McGuire, “Study of exactly solvable one-dimensional  $N$ -body problems,” *J. Math. Phys.* **5** (1964) 622–636.
- [4] C. N. Yang, “Some exact results for the many-body problem in one dimension with repulsive delta-function interaction,” *Phys. Rev. Lett.* **19** (1967) 1312–1315.
- [5] R. J. Baxter, “Partition function of the eight-vertex lattice model,” *Ann. Physics* **70** (1972) 193–228.
- [6] M. Kashiwara, and T. Miwa, A class of elliptic solutions to the star-triangle relation. *Nucl. Phys. B* **275** (1986) 121–134.
- [7] G. von Gehlen and V. Rittenberg,  $Z(n)$ -symmetric quantum chains with an infinite set of conserved charges and  $Z(n)$  zero modes. *Nucl. Phys. B* **257** (1985) 351.

- [8] H. Au-Yang, B. M. McCoy, J. H. H. Perk, S. Tang and M. L. Yan, “Commuting transfer matrices in the chiral Potts models: Solutions of Star triangle equations with genus  $> 1$ ”, *Phys. Lett. A* **123** (1987) 219–223.
- [9] R. J. Baxter, J. H. H. Perk and H. Au-Yang, “New solutions of the star triangle relations for the chiral Potts model”, *Phys. Lett. A* **128** (1988) 138–142.
- [10] V. A. Fateev and A. B. Zamolodchikov, Self-dual solutions of the star-triangle relations in  $Z_N$ -models. *Phys. Lett. A* **92** (1982) 37–39.
- [11] R. J. Baxter, A rapidity-independent parameter in the star-triangle relation. In *Math-Phys Odyssey, 2001, Prog. Math. Phys.*, **23**, 9–63. Birkhäuser Boston, Boston, MA, 2002, [arXiv:cond-mat/0108363](#).
- [12] A. B. Zamolodchikov, “Fishing-net” diagrams as a completely integrable system. *Phys. Lett. B* **97** (1980) 63–66.
- [13] A. Y. Volkov, and L. D. Faddeev, Yang-Baxterization of the quantum dilogarithm. *Zapiski Nauchnykh Seminarov POMI* **224** (1995) 146–154. English translation: *J. Math. Sci.* **88** (1998) 202–207.
- [14] V. V. Bazhanov, V. V. Mangazeev, and S. M. Sergeev, Faddeev-Volkov solution of the Yang-Baxter Equation and Discrete Conformal Symmetry. *Nucl. Phys. B* **784** (2007) 234–258, [arXiv:hep-th/0703041](#).
- [15] A. I. Bobenko, and B. A. Springborn, Variational principles for circle patterns and Koebe’s theorem. *Trans. Amer. Math. Soc.* **365** (2004) 659–689, [arXiv:math/0203250](#).
- [16] K. Stephenson, *Introduction to circle packing. The theory of discrete analytic functions*. Cambridge University Press, Cambridge, 2005.
- [17] V. E. Adler, A. I. Bobenko, and Y. B. Suris, Classification of integrable equations on quad-graphs. The consistency approach. *Comm. Math. Phys.* **233** (2003) 513–543, [arXiv:nlin/0202024](#).
- [18] V. V. Bazhanov and S. M. Sergeev, A master solution of the quantum Yang-Baxter equation and classical discrete integrable equations, *Adv. Theor. Math. Phys.*, **16** (2012) 65 – 95, [arXiv:1006.0651](#).
- [19] L. Faddeev, Modular double of a quantum group, in *Conférence Moshé Flato 1999, Vol. I (Dijon)*, vol. 21 of *Math. Phys. Stud*, pp. 149–156. Kluwer Acad. Publ., Dordrecht, 2000, [arXiv:math/9912078](#)
- [20] V. P. Spiridonov, Essays on the theory of elliptic hypergeometric functions, *Uspekhi Mat. Nauk* **63** (2008) no. 3(381), 3–72, [arXiv:0805.3135](#).
- [21] E. K. Sklyanin, Some algebraic structures connected with the Yang-Baxter equation, *Func. Anal. Appl.* **16** (1982) no. 4, 263–270.
- [22] V. P. Spiridonov, On the elliptic beta function. *Uspekhi Mat. Nauk* **56** (1) (2001) 181–182. English translation: *Russ. Math. Surveys* **56** (1) (2001) 185–186.
- [23] V. V. Bazhanov and Y. G. Stroganov, Chiral Potts model as a descendant of the six vertex model, *J. Statist. Phys.* **59** (1990) 799–817.
- [24] H. Au-Yang and J. H. H. Perk, Integrable Chiral Potts Model and the Odd-Even Problem in Quantum Groups at Roots of Unity. [arXiv:1806.03359](#).
- [25] R. J. Baxter, V. V. Bazhanov and J. H. H. Perk, Functional relations for transfer matrices of the chiral Potts model. *Internat. J. Modern Phys. B* **4** (1990) 803–870.

- [26] N. M. Vildanov, Some extensions of Ramanujan’s  ${}_1\psi_1$  summation formula. [arXiv:1204.6569](#).
- [27] S. Garoufalidis and R. Kashaev, A meromorphic extension of the 3D Index, *Res Math Sci* **6** (2019) 8, [arXiv:1706.08132](#).
- [28] V. V. Bazhanov, R. M. Kashaev, V. V. Mangazeev and Y. G. Stroganov, “ $(Z_N)^{\otimes(n-1)}$  generalization of the chiral Potts model”, *Comm. Math. Phys.* **138** (1991) 393–408.
- [29] V. V. Bazhanov and S. M. Sergeev, An Ising-type formulation of the six-vertex model, *Nucl. Phys. B* **986** (2023) 116055, [arXiv:2205.10708](#).
- [30] L. D. Faddeev and R. M. Kashaev, Quantum Dilogarithm, *Mod. Phys. Lett. A* **9** (1994) 427–434, [arXiv:hep-th/9310070](#).
- [31] V. V. Bazhanov and R. J. Baxter, Star triangle relation for a three-dimensional model, *J. Statist. Phys.* **71** (1993) 839–864, [arXiv:hep-th/9212050](#).
- [32] R. J. Baxter, Solvable eight-vertex model on an arbitrary planar lattice. *Philos. Trans. Roy. Soc. London Ser. A* **289** (1978) 315–346.
- [33] R. J. Baxter, Functional relations for the order parameters of the chiral Potts model. *J. Statist. Phys.* **91** (1998) 499–524, [arXiv:cond-mat/9808120](#).
- [34] Y. G. Stroganov, A new calculation method for partition functions in some lattice models. *Phys. Lett. A* **74** (1979) 116–118.
- [35] A. B. Zamolodchikov,  $Z_4$ -symmetric factorized  $S$ -matrix in two space-time dimensions. *Comm. Math. Phys.* **69** (1979) 165–178.
- [36] R. J. Baxter, The inversion relation method for some two-dimensional exactly solved models in lattice statistics. *J. Statist. Phys.* **28** (1982) 1–41.
- [37] V. V. Bazhanov, A. P. Kels and S. M. Sergeev, Quasi-classical expansion of the star-triangle relation and integrable systems on quad-graphs, *J. Phys. A* **49**, no.46 (2016) 464001, [arXiv:1602.07076](#).
- [38] D. Chicherin, V. Kazakov, F. Loebbert, D. Müller and D. I. Zhong, Yangian Symmetry for Bi-Scalar Loop Amplitudes, *JHEP* **05** (2018) 003, [arXiv:1704.01967](#).
- [39] V. Kazakov, F. Levkovich-Maslyuk and V. Mishnyakov, Integrable Feynman Graphs and Yangian Symmetry on the Loom, [arXiv:2304.04654](#).
- [40] C. Fan and F. Y. Wu, General Lattice Model of Phase Transitions, *Phys. Rev. B* **2** (1970) 723–733.
- [41] B. U. Felderhof, Diagonalization of the transfer matrix of the free-fermion model II, *Physica* **66** (1973) 279–297.
- [42] V. V. Bazhanov and Y. G. Stroganov, Hidden Symmetry of the Free Fermion Model. 2. Partition Function, *Theor. Math. Phys.* **63** (1985) 519.
- [43] R. J. Baxter, Free-fermion, checkerboard and Z-invariant lattice models in statistical mechanics, *Proc. Roy. Soc. Lond. A* **404** (1986) 1–33
- [44] H. Au-Yang and J. H. H. Perk, The large- $N$  limits of the chiral Potts model, *Physica A* **268** (1999) 175–206, [arXiv:math/9906029](#).
- [45] V. G. Drinfel’d, Quantum groups. In *Proceedings of the International Congress of Mathematicians, Vol. 1, 2* (Berkeley, Calif., 1986), pages 798–820, Providence, RI, 1987. Amer. Math. Soc.; *J. Math. Sci.* **41** (1988) 898–915.

- [46] M. Jimbo, “A  $q$ -analogue of  $U(\mathfrak{gl}(N + 1))$ , Hecke algebra, and the Yang-Baxter equation,” *Lett. Math. Phys.* **11** (1986) 247–252.
- [47] L. D. Faddeev, N. Y. Reshetikhin and L. A. Takhtajan, Quantization of Lie Groups and Lie Algebras, *Alg. Anal.* **1** (1989) 178-206.
- [48] M. Caselle, A. Nada, M. Panero and D. Vadicchino, Conformal field theory and the hot phase of three-dimensional  $U(1)$  gauge theory, *JHEP* **05** (2019) 068, [arXiv:1903.00491](https://arxiv.org/abs/1903.00491).
- [49] V. L. Berezinskii, Destruction of long-range order in one-dimensional and two-dimensional systems having a continuous symmetry group I. Classical systems, *Sov. Phys. JETP*, **32**(3) (1971) 493–500.
- [50] J. M. Kosterlitz and D. J. Thouless, Ordering, metastability and phase transitions in two-dimensional systems, *J. Phys. C: Solid State Phys.*, **6** (7) (1973) 1181–1203.